BMC Biology

RESEARCH ARTICLE

Open Access

From birth to bite: the evolutionary ecology of India's medically most important snake venoms

R. R. Senji Laxme[1], Suyog Khochare[1], Siddharth Bhatia[1], Gerard Martin[2] and Kartik Sunagar[1*]

Abstract

Background Snake venoms can exhibit remarkable inter- and intraspecific variation. While diverse ecological and environmental factors are theorised to explain this variation, only a handful of studies have attempted to unravel their precise roles. This knowledge gap not only impedes our understanding of venom evolution but may also have dire consequences on snakebite treatment. To address this shortcoming, we investigated the evolutionary ecology of venoms of Russell's viper (*Daboia russelii*) and spectacled cobra (*Naja naja*), India's two clinically most important snakes responsible for an alarming number of human deaths and disabilities.

Methodology Several individuals ($n=226$) of *D. russelii* and *N. naja* belonging to multiple clutches ($n=9$) and their mothers were maintained in captivity to source ontogenetic stage-specific venoms. Using various in vitro and in vivo assays, we assessed the significance of prey, ontogeny and sex in driving venom composition, function, and potency.

Results Considerable ontogenetic shifts in venom profiles were observed in *D. russelii*, with the venoms of newborns being many times as potent as juveniles and adults against mammalian (2.3–2.5×) and reptilian (2–10×) prey. This is the first documentation of the ontogenetic shift in viperine snakes. In stark contrast, *N. naja*, which shares a biogeographic distribution similar to *D. russelii*, deployed identical biochemical cocktails across development. Furthermore, the binding kinetics of cobra venom toxins against synthetic target receptors from various prey and predators shed light on the evolutionary arms race.

Conclusions Our findings, therefore, provide fascinating insights into the roles of ecology and life history traits in shaping snake venoms.

Keywords Ontogenetic shift, Evolutionary ecology, Snake venom, Prey-specific toxicity, Snakebite therapy

Background

Venom is an intrinsically ecological trait that enables venom-producing animals to incapacitate prey, outcompete conspecifics, deter predators or a combination thereof [1, 2]. As a result, venom toxins are theorised to coevolve with their interacting partners [1, 2]. Snake venoms, in particular, are well-known to exhibit considerable inter- and intraspecific variation in composition, function and potency that is largely driven by their evolutionary ecology [1]. Numerous factors, including climatic conditions, sexual dimorphism, dietary specialisation, predator pressures and ontogenetic shifts, have been invoked to explain venom variation in snakes [2, 3]. However, studies investigating the importance of these factors in shaping snake venoms have been limited. This

*Correspondence:
Kartik Sunagar
ksunagar@iisc.ac.in
[1] Evolutionary Venomics Lab, Centre for Ecological Sciences, Indian Institute of Science, Bangalore 560012, Karnataka, India
[2] The Liana Trust. Survey, #1418/1419 Rathnapuri, Hunsur 571189, Karnataka, India

is especially true for the medically most important snakes of the Indian subcontinent that are responsible for a vast number of human envenomings, deaths and disabilities [4, 5].

Studies in the past have highlighted the effect of intraspecific venom variation on the clinical manifestations of envenomings and the efficiency of commercial polyvalent antivenoms in treating snakebite [6–14]. For instance, Russell's viper envenomings are often associated with severe local necrosis, venom-induced consumptive coagulopathy (VICC), nephrotoxicity and systemic haemorrhage [15, 16]. However, certain populations of this species have also been reported to inflict peripheral arterial thrombosis [17], neuromuscular paralysis [18] and bilateral blindness [19] in rare instances owing to the compositional variation. While the spectacled cobra envenomings are characterised by systemic neurotoxicity, local dermonecrosis and myonecrosis are also observed in certain regions [6, 20]. These variations in the clinical symptoms, combined with the lack of broadly effective antivenoms, serve as a major hurdle for the clinical management of snakebites. Therefore, understanding the evolutionary ecology of venoms is crucial for the design of a broadly effective snakebite therapy, particularly in regions that suffer the highest burden of snakebite [1].

To address this knowledge gap, we assessed the roles of various ecological and evolutionary processes in shaping the venoms of Russell's viper (*Daboia russelii)* and spectacled cobra (*Naja naja*)—two snake species that collectively contribute the highest number of snakebite-related deaths and disabilities in India. By comparatively assessing their venom proteomes, biochemical and pharmacological functions, receptor-toxin interactions and venom potencies against a variety of prey and predatory animals, we evaluated the roles of sex, ontogeny and evolutionary arms race in shaping the venoms of these snakes. Our findings highlight, for the first time, how distinct ecological and evolutionary forces have influenced the venoms of India's medically most important snakes.

Results

Proteomic composition of young and adult snake venoms

Electrophoretic profiles of *D. russelii* and *N. naja* venoms from various developmental stages provided interesting insights into ontogenetic venom variation (Fig. 1; Additional file 1: Fig S1–2). The venoms of *D. russelii* adults (mothers and unrelated males) were enriched with high-molecular-weight (HMW; 50–70 kDa) toxins, whereas the venoms of neonates and juveniles were rich in low-molecular-weight (LMW; 10–15 kDa) toxins. Prominent LMW bands (2–5 kDa) were also noted in adults but were less abundant in neonates and juveniles (Fig. 1A; Additional file 1: Fig S1). While the differences in venom sodium dodecyl sulphate–polyacrylamide gel electrophoresis (SDS-PAGE) profiles were more pronounced in *D. russelii,* only subtle differences were observed in the venoms of juvenile and adult *N. naja* (Fig. 1B). Interestingly, inter-individual differences in the intensities of bands corresponding to LMW toxins (2–10 kDa) were also noted in the venoms of juvenile individuals of *N. naja* sampled from the same clutch (J1–J22; Fig. 1B; Additional file 1: Fig S2). A similar pattern was observed in the venoms of neonates and juveniles collected from different clutches of *D. russelii* (Additional file 1: Fig S1). When the venoms of juvenile *D. russelii* snakes, periodically collected

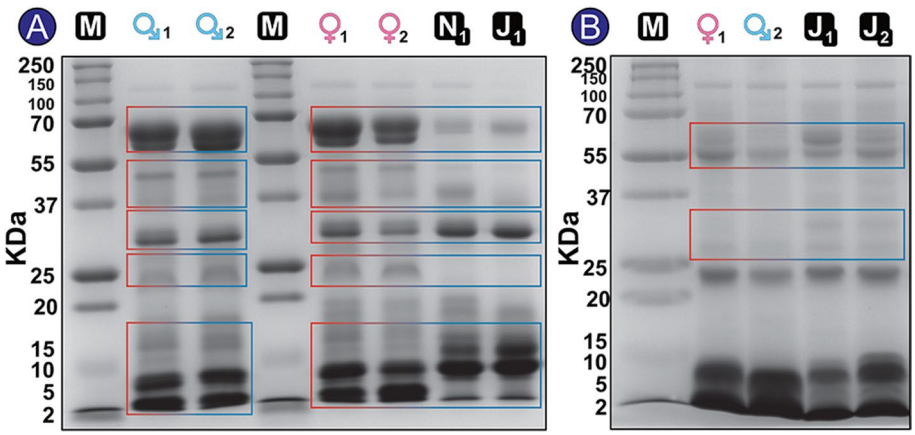

Fig. 1 SDS-PAGE venom profiles of ontogenetic stages of *D. russelii* and *N. naja*. The figures depict the SDS-PAGE profiles of (**A**) *D. russelii* and *N. naja* (**B**) venoms (replicate $n = 1$). The highlighted regions represent the major differences between the venom profiles. Relationships of individuals from which the venoms were collected and pooling information are provided in Additional file 2: Tables 1 and 2. M standard protein ladder, ♂ unrelated male, ♀ adult mother, N neonate, J juvenile

every 3 months, were analysed, a distinct shift in venom phenotype was recorded between 6 and 9 months (Additional file 1: Fig S1D). The venom profile of 9-month-old juveniles resembled the adult profile, with a prominent HMW band around 70 kDa. The venoms of juvenile *N. naja* were also collected every 3 months up to a year, but noticeable ontogenetic shifts were not observed in distinct clutches (Additional file 1: Fig S2). To understand the influence of sex, the venom profiles of unrelated adult male and female *D. russelii* and *N. naja* were compared (Additional file 1:Fig S3). However, prominent sex-specific differences in the SDS-PAGE banding patterns were not observed.

Additionally, *D. russelii* venoms were also subjected to RP-HPLC (Fig. 2). Considering the lack of sufficient amounts of venoms from the early developmental stages, and the high replicability of Reversed-phase high-performance liquid chromatography (RP-HPLC) experiments (Additional file 1: Fig S4), we generated a single fractionation profile for each venom. Here, neonate, juvenile and adult venoms separated into 12, 14 and 16 fractions, respectively. These fractions were subsequently subjected

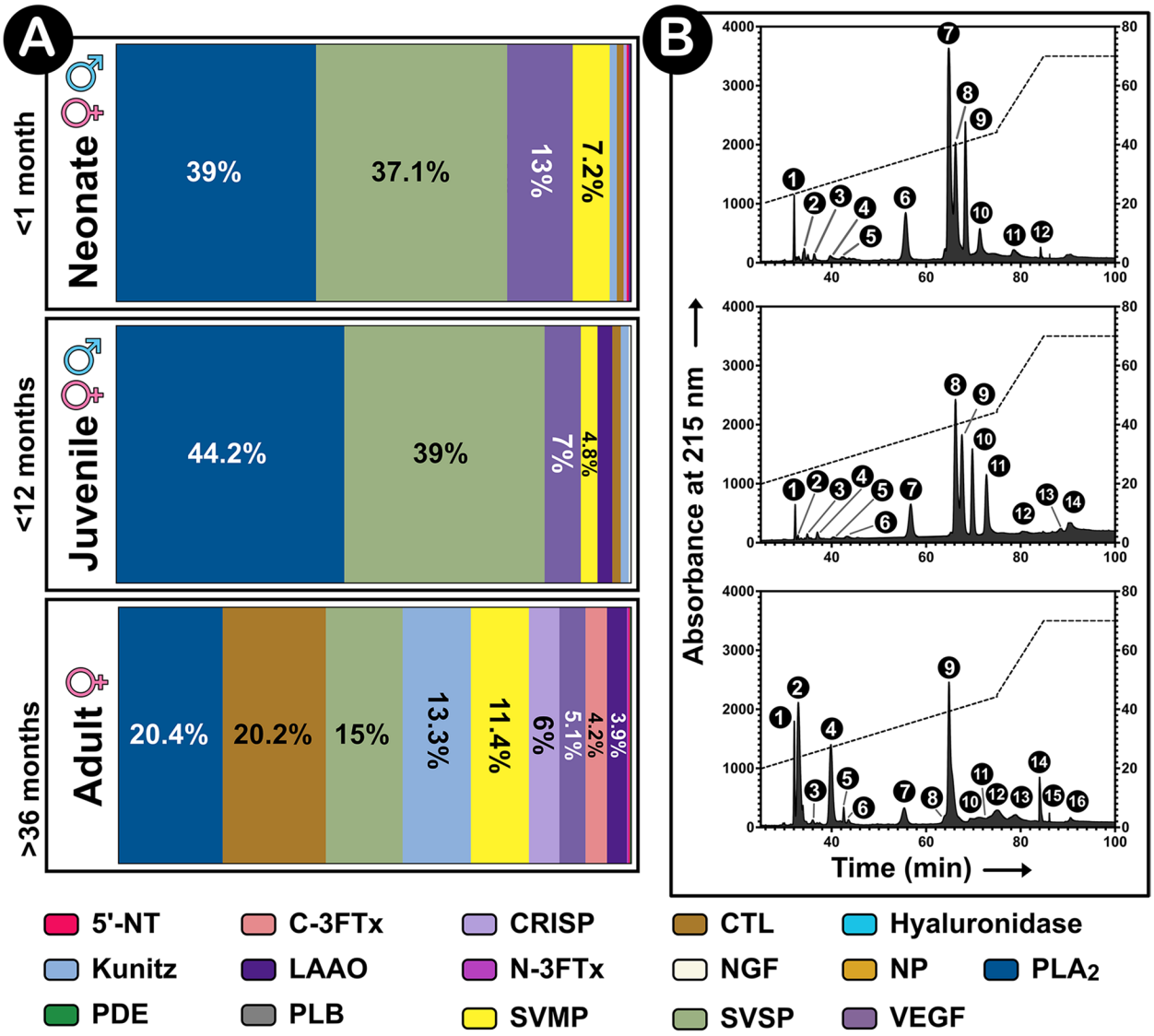

Fig. 2 Ontogenetic shift in the venom proteomic composition of Russell's viper. This figure depicts the **A** relative proteomic abundance and **B** RP-HPLC profiles corresponding to the ontogenetic stages (neonate, juvenile and adult) of *D. russelii*. The relative abundance of toxin families, determined by tandem mass spectrometry, is shown as parts of the whole graph on the left. RP-HPLC profiles ($n = 1$) corresponding to each developmental stage, where the absorbance at 215 nm (*y*-axis) is plotted against elution time (*x*-axis) in minutes, are shown on the right. The supporting data are provided in Additional file 2: Table S2A-S2C

to SDS-PAGE (Additional file 1: Fig S5), followed by in-gel digestion and mass spectrometry. In RP-HPLC profiles, the prominent peaks that eluted around the 30th minute (peaks 1–3) in the adult venom were negligible in both neonate and juvenile *D. russelii* venoms. When we subjected these fractions from adult venoms to LC–MS/MS, we detected C-type lectins (CTL), cytotoxic three-finger toxins (C-3FTx) and disintegrins (Additional file 2: Table S2A; Additional file 4). Similarly, the other major peak around the 40th minute (peaks 4–6) in the adult venom, which contained Kunitz-type serine protease inhibitors (Kunitz) and Phospholipases (PLA_2s), was negligible in the venoms of the younger stages. Likewise, the 84th-minute peak 14 corresponding to snake venom metalloproteinase (SVMP) was also negligible in the younger stages. Venoms were separated into four fractions between 60 and 80 min for neonates (peaks 7–11) and juveniles (peaks 8–11), whereas a single prominent peak (#9) was detected in the adult venom. We recovered PLA_2, snake venom serine protease (SVSP) and vascular endothelial growth factor (VEGF) toxin families from these peaks of neonates and juveniles (Additional file 2: Table S2B and S2C; Additional file 4). The same toxin families were also recovered from the corresponding peak (peak #9) in adult venoms. Overall, in terms of the number of RP-HPLC fractions recovered, the venom of the adult *D. russelii* appeared to be more complex than that of neonate and juvenile individuals. The major toxin families detected in adult venoms included PLA_2 (20.4%), CTL (20.2%), SVSP (15%), Kunitz (13.3%) and SVMP (11.4%), whereas neonates and juveniles had PLA_2 (~39–44.2%) and SVSP (~39%). Minor toxin families identified in adult venoms included cysteine-rich secretory proteins (CRISP) (6%), VEGF (5.1%), C-3FTx (4.2%) and L-amino acid oxidase (LAAO; 3.9%). In the case of neonates and juveniles, minor toxin families included SVMP (~4.8–7.2%), CTL (~1%) and Kunitz (~1%). The abundance of neurotoxic three-finger toxins (N-3FTx), 5'-nucleotidase (5'-NT), phosphodiesterase (PDE), nerve growth factor (NGF) and hyaluronidase was less than 1% in adult venoms. Similarly, NGF, C-3FTx and 5'-NT were detected in both neonates and juveniles, and their proportions were lower than 1% of the whole venom. Additionally, PDE, hyaluronidase, natriuretic peptides (NP) and phospholipase B (PLB) were only detected in neonates in negligible amounts. Overall, the venom profile of *D. russelii* was consistent with previous reports and was largely dominated by PLA_2, SVMP and SVSP toxins [21–26]. Previously, N-3FTx and C-3FTx transcripts have been identified from the venom gland transcriptomes of viperid snakes [27–30]. Similarly to a few reports ([7, 31, 32]), we were also able to recover these 3FTx variants from the venom proteome of *D. russelii*. While it is unlikely that 3FTxs play any major role in *Daboia* envenoming/prey capture, their venom gland expression reflects on the recruitment of this toxin type at the base of Caenophidia and Henophidia [33].

In contrast to the stark ontogenetic shifts observed in *D. russelii*, RP-HPLC venom profiles of *N. naja* juveniles and their adult mother revealed lesser differences as they resolved into 14 and 12 peaks, respectively. A major difference was seen in the peak that eluted at the 44th minute (peaks 4–6) in the adult *N. naja* venom, where a higher peak area was documented compared to corresponding elution in juveniles (Fig. 3). Although the elution profiles of fractions between 60 and 70 min were similar in juvenile (peaks 10–12) and adult venoms (peaks 9 and 10), their proteomic composition varied (Fig. 3, Additional file 2: Table S2D and S2E; Additional file 4). The difference in the proteomic profiles was majorly due to the abundance of CRISPs in juveniles and C-3FTx in adults. While the major components in juvenile *N. naja* venoms were CRISPs (30%), N-3FTx (24.4%) and C-3FTx (16%), the venom of their adult mother was chiefly composed of C-3FTx (64%) and N-3FTx (26.5%). Minor toxin families documented in juveniles were Kunitz (7.4%), PLA_2 (6.3%), LAAO (6%), SVSP (4.4%) and SVMP (1.8%), whereas Kunitz (4.9%) and CRISP (1%) were identified in the adult female. LAAO, PLA_2, cobra venom factor (CVF), SVMP, CTL, PDE, acetylcholinesterase (ACE) and 5'-NT were less than 1% in adult venoms, whereas in the case of juveniles, NGF, Vespryn and CVF constituted less than 1%.

As we could only source very small amounts of venoms (5 µl) from neonates of *N. naja*, the RP-HPLC, mass spectrometry and other functional and toxinological comparisons could not be performed. However, marked differences were not observed in the venom SDS-PAGE profiles of neonates and juveniles of this species (Additional file 1: Fig S2).

Biochemical assessment of toxin functions

To assess the impact of compositional variation of *D. russelii* venom on its function, several biochemical assays were conducted. The venoms of younger stages exhibited relatively higher PLA_2 activity (~400 nmol/mg/min) than the venoms of adults (~100 nmol/mg/min; $p < 0.0001$; Fig. 4A). When the proteolytic activities of young and adult *D. russelii* venoms were evaluated, the adult venoms exhibited higher proteolysis (>30%) compared to the younger individuals (0 to 1%; $p < 0.0001$; Fig. 4B). Preincubation of adult venoms with ethylenediaminetetraacetic acid (EDTA) inhibited the cleavage of azocasein, but phenylmethylsulfonyl fluoride (PMSF) treatment did not affect the venom activity. These results are in line with the relative proteomic

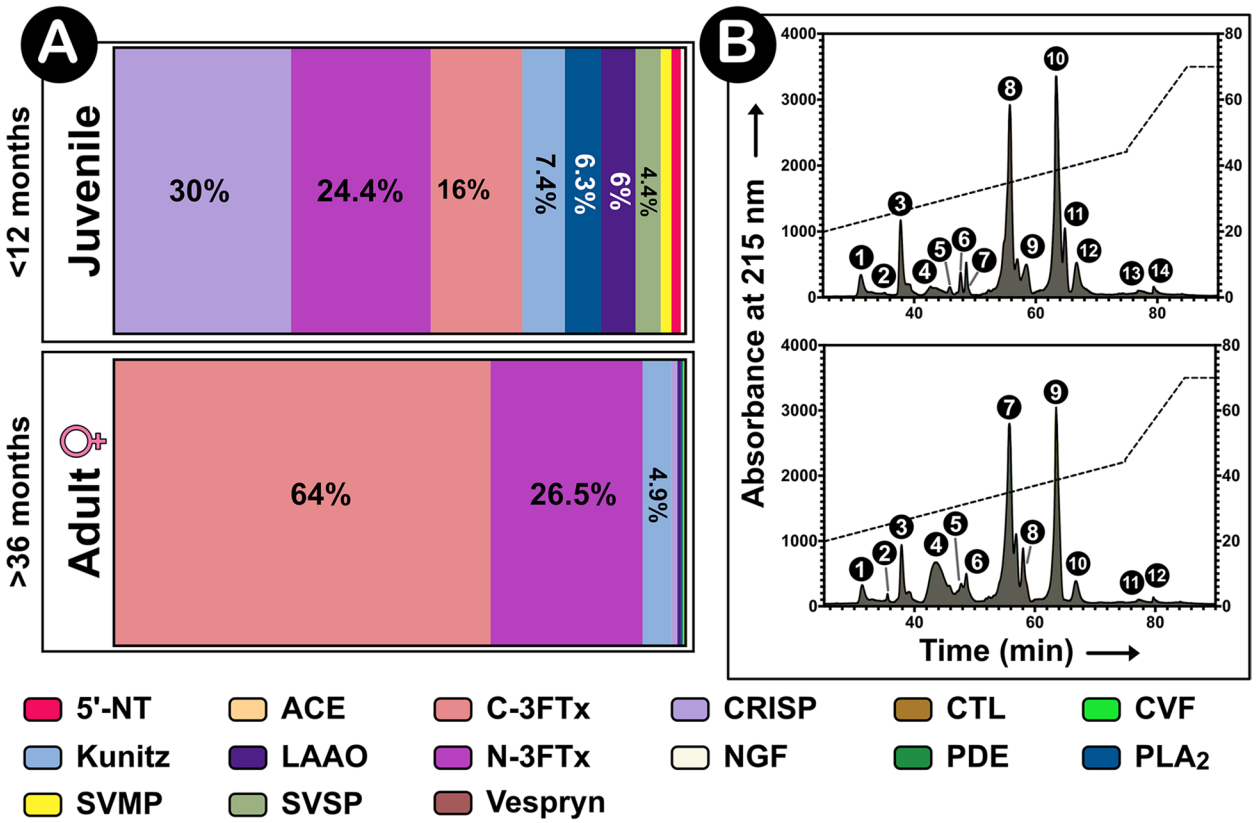

Fig. 3 Ontogenetic shift in the venom proteomic composition of spectacled cobra. This figure depicts the **A** relative proteomic abundance and **B** RP-HPLC profiles corresponding to the ontogenetic stages (juvenile and adult) of *N. naja*. The relative abundance of toxins, determined by tandem mass spectrometry, is shown as parts of the whole graph on the left. RP-HPLC profiles ($n = 1$) corresponding to each developmental stage, where the absorbance at 215 nm (*y*-axis) is plotted against elution time (*x*-axis) in minutes, are shown on the right. The supporting data are provided in Additional file 2: Table S2D-S2E

abundance of PLA_2s and SVMPs in the venoms of younger and adult individuals. The venoms of younger *D. russelii* also induced higher direct haemolysis in comparison to the adult venoms that lacked quantifiable haemolytic activity ($p < 0.0001$; Fig. 4C). In addition, when tested for their ability to cause deamination of L-amino acid substrates, the adult *D. russelii* venoms exhibited relatively higher activity in comparison to the venoms of younger stages ($p < 0.0001$; Fig. 4D). Similar patterns were observed for all the neonate and juvenile venoms collected from various clutches (Additional file 1: Fig S6). Consistent with the SDS-PAGE profile, venoms collected from the 9-month-old juvenile *D. russelii* snakes exhibited functional activities similar to that of the adults. The venoms of both the younger and adult stages resulted in the cleavage of the Aα human fibrinogen chain, which was, in turn, inhibited by the addition of either EDTA or PMSF (Additional file 1: Fig S7A). The Clauss fibrinogen quantification assay revealed that the fibrinogen concentrations in plasma (control—251.85 mg/dl) treated with the venoms of younger stages were significantly lower than the plasma treated with the adult venoms ($p < 0.0001$; Fig. 4E). Interestingly, the juvenile *D. russelii* venom reduced the fibrinogen concentration to as low as 30 mg/dl from an initial concentration of 252 mg/dl (control plasma), while the venoms of neonate and adult stages reduced the fibrinogen concentration to 70 mg/dl and ~ 160 mg/dl, respectively (Fig. 4E).

When the venoms of juvenile and adult *N. naja* were tested, their functional profiles did not exhibit prominent differences, which was consistent with their venom proteomic compositions (Figs. 4F–G). While the venoms of juvenile *N. naja* exhibited slightly lower PLA_2 activity (34–40 nmol/mg/min) than that of the adults (81–104 nmol/mg/min; $p < 0.0001$), the LAAO activity of juvenile venoms (1762–2389 nmol/mg/min) was comparatively higher than adults (775–849 nmol/mg/min; $p < 0.0001$). Additionally, notable differences were not observed in the fibrinogenolytic activities of *N. naja* venoms (Additional file 1: Fig S7B).

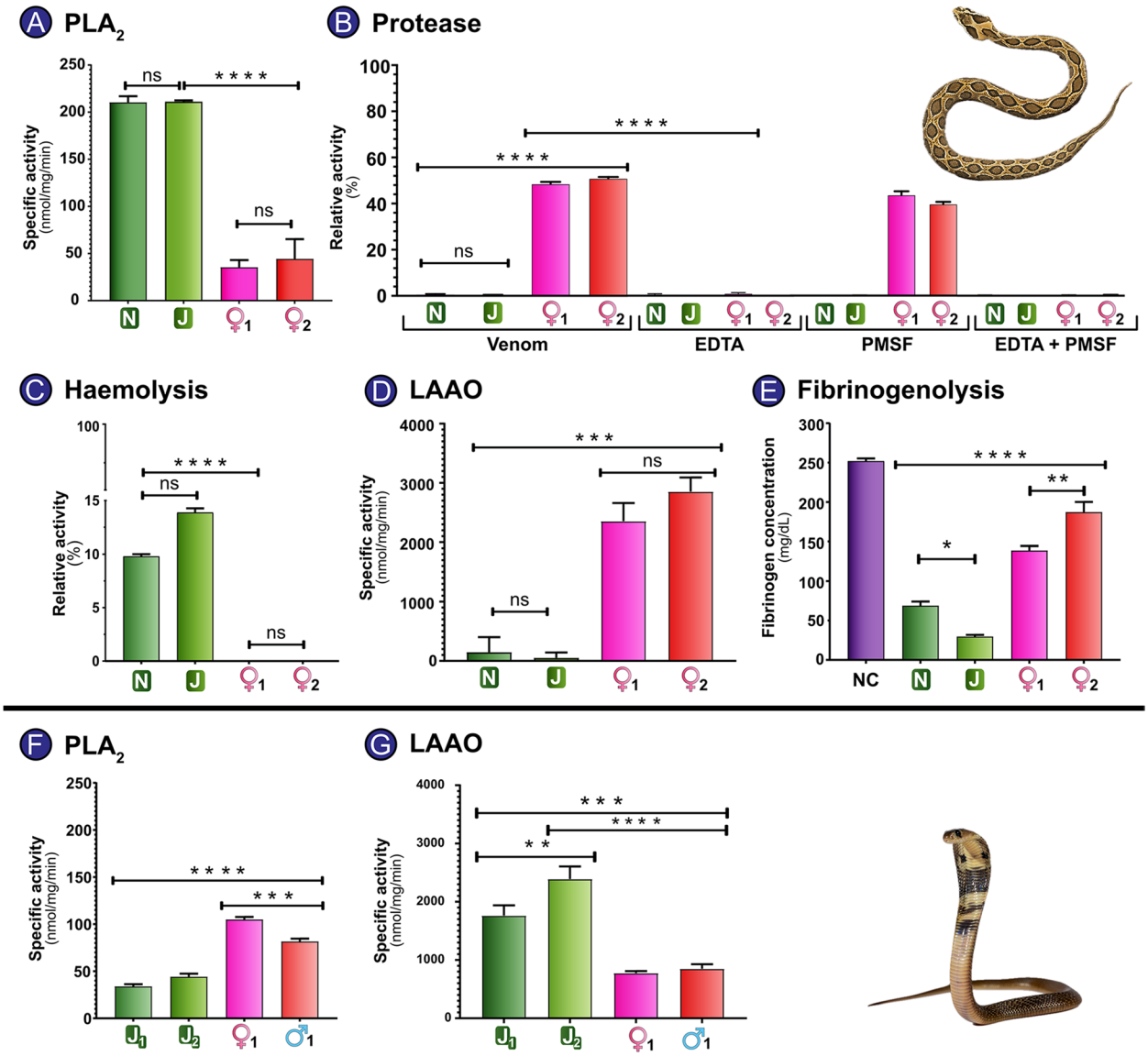

Fig. 4 Enzymatic activities of venoms of young and adult stages of *D. russelii* and *N. naja*. This figure depicts PLA_2 (**A** and **F**), proteolytic (with and without SVMP and SVSP inhibitors) (**B**), haemolytic (**C**), LAAO (**D** and **G**), and fibrinogenolytic activities (**E**) of venoms of young and adult *D. russelii* (**A**–**E**) and *N. naja* (**F**–**G**). In these figures, the mean activities of replicates ($n = 3$) are provided, and the standard deviation is represented as error bars. NC negative control, PC positive control, N neonate, J juvenile, and ♀ adult mother. The activities of the young and adult venoms are compared using one-way ANOVA. The statistical significance is represented as follows: $p < 0.01$ and $p < 0.0001$ are indicated as ** and ****, respectively. ns indicates statistical insignificance. The supporting data are provided in Additional File 3

Acetylcholine receptor specificity of venoms

Since non-enzymatic 3FTxs constitute a major proportion of *N. naja* venoms, their binding kinetics against synthetic nicotinic acetylcholine receptors (nAChRs; α1-subtype) from various organisms, including prey and predators of *N. naja*, was assessed. Here, the wavelength shift or the increase in thickness of the molecular layer on streptavidin sensor tips, resulting from the interaction between the venoms and biotinylated nAChR mimotopes, was recorded and plotted against time (Fig. 5; Additional file 1: Fig S8). The association phase is defined as the time interval during which the analyte interacts with the mimotope molecules. In contrast, the dissociation phase represents the time when the neurotoxin-receptor complexes bound to streptavidin sensor tips dissociate into the assay buffer in the absence of the analyte. The area under the curve (AUC) comparison of the association and dissociation kinetics demonstrated

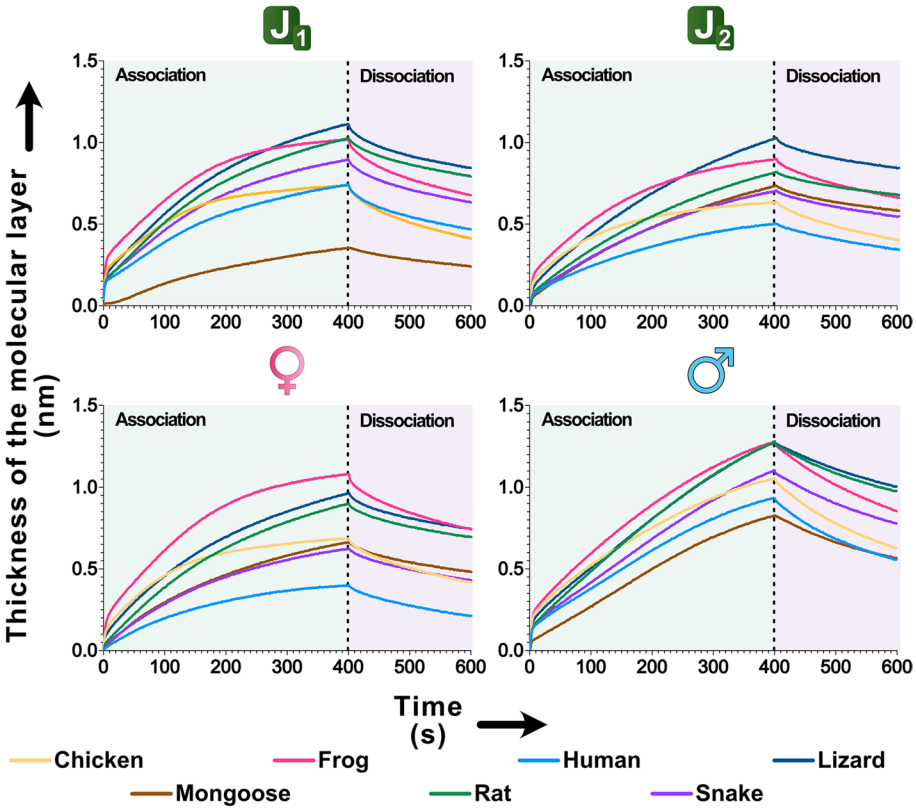

Fig. 5 Binding kinetics of *N. naja* venoms towards α1-nAChRs. In this figure, the binding kinetics of *N. naja* venoms from young and adult stages are depicted as line graphs (replicate $n = 1$). Here, the thickness of the molecular layer corresponding to the binding strength of venom toxins to α1-nAChRs from various organisms, including prey and predators of *N. naja*, is plotted against time (s). The dotted line at 400 s represents the demarcation between the association and dissociation phases. J_1 and J_2 juvenile venoms, ♂ unrelated male, ♀ adult mother of the juveniles. The AUC comparisons for association and dissociation kinetics are provided in Additional file 1: Fig S8. The supporting data are provided in Additional File 3

that *Naja* venoms, irrespective of whether they were from juveniles or adults, exhibited increased binding towards rat, frog and lizard nAChRs in comparison to snake and chicken receptors ($p < 0.05$; Additional file 1: Fig S8). However, venoms of both juvenile and adult *N. naja* bound the least to the receptors of mongooses and humans. Further, in the case of juvenile J2 and its adult female, the binding against the mongoose receptor was also similar to that of chicken and snake receptors ($p > 0.05$), with the binding against human receptors being the lowest. *N. naja* venoms exhibited 25% higher binding towards amphibian nAChRs than other receptors, while they exhibited 66% lower binding towards mongoose nAChRs (Fig. 5; Additional file 1: Fig S8).

Lethal potencies of venoms across developmental stages

The median lethal doses (LD_{50}) of *D. russelii* venoms varied across their developmental stages (Fig. 6A; Additional File 2: Table S5A). The venoms of adult (0.166 mg/kg) and juvenile (0.176 mg/kg) *D. russelii* from Karnataka exhibited potencies similar to that of adults from other populations across India (0.1–0.3 mg/kg; [7, 34]). However, the venoms of neonates exhibited extremely high venom potency against mice (LD_{50} of 0.072 mg/kg), which was comparable to that of certain krait venoms [5, 10, 35]. In contrast, venoms of *N. naja* juvenile (0.380 mg/kg) and adult (0.363 mg/kg) stages had a venom potency that was similar to the pan-Indian *N. naja* populations Fig. 6A; Additional File 2: Table S6A; [6, 9, 36]. Interestingly, a similar trend was observed in assays involving house geckos, where neonate *D. russelii* venoms were found to be extremely potent (2.024 mg/kg). The venom of juveniles killed 50% of the test population at ~ 4 mg/kg. In both cases, geckos were paralysed and lost the righting reflex within 30 min of venom injection. On the contrary, though the adult *Daboia* venoms induced partial paralysis during the initial hours of experimentation (2–4 h), venom-injected geckos eventually recovered completely, even at doses as high as 20 mg/kg (Fig. 6B; Additional File 2: Table S5B). Not surprisingly, *N. naja* venoms exhibited higher lethal potencies against geckos in comparison to *D. russelii*. LD_{50} of 0.510 and

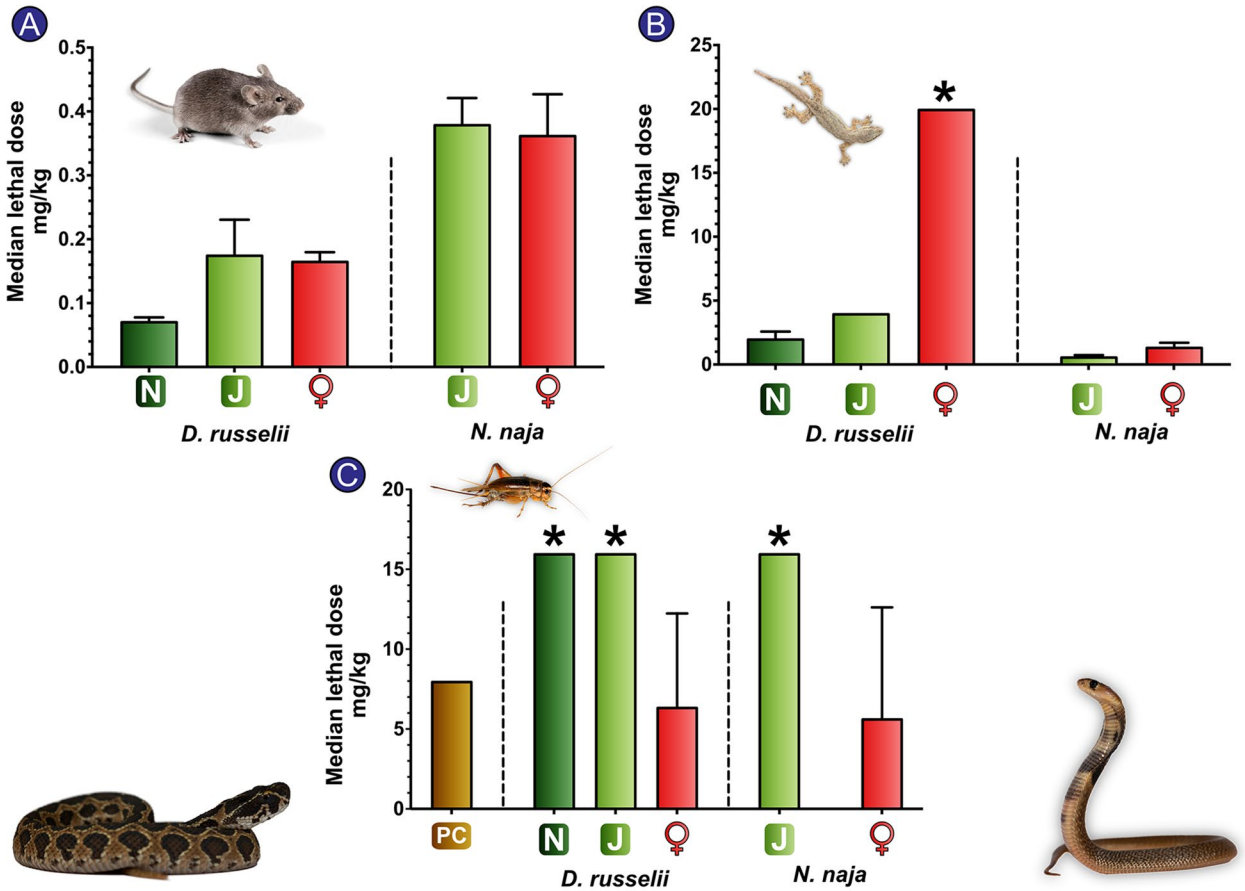

Fig. 6 Toxicity profiles of ontogenetic stages of *D. russelii* and *N. naja*. Bar graphs in this figure represent the LD_{50} (mg/kg) of the young and adult *D. russelii* and *N. naja* venoms against **A** mouse, **B** gecko and **C** cricket. N neonate, J juvenile, ♂ unrelated male, ♀ adult mother, PC positive control (*H. tamulus* venom); asterisk indicates absence of lethality at the highest tested concentration. The error bars indicate 95% confidence interval (CI) calculated using Probit statistics. Representative photographs of neonate *D. russelii* and *N. naja* are also shown. Detailed information on venom doses (µg), number of test animals, survival patterns and LD_{50} with 95% CI are provided in Additional file 2: Tables S5 and S6

1.265 mg/kg were recorded for adult and juvenile venoms, respectively (Fig. 6B; Additional File 2: Table S6B). However, unlike ontogenetic shifts in venom potency documented in *D. russelii*, a significant shift was not observed in *N. naja*. When the *D. russelii* venoms were tested on crickets, neonate and juvenile venoms did not exhibit any toxicity at concentrations as high as 16 mg/kg (Fig. 6C; Additional File 2: Table S5C). Surprisingly, though the adult venom did not induce instant paralysis, it was lethal to crickets at a concentration of 6.375 mg/kg several hours post-venom injection. When similar experiments were conducted with scorpion venoms, crickets were paralysed within 5 min of injection and lethality was observed at doses as low as 2.828 mg/kg (Fig. 6C; Additional File 2: Table S5C). Both adult and juvenile *N. naja* venoms did not induce paralysis in crickets, and only the adult venoms killed crickets (LD_{50} of 5.657 mg/kg) several hours post-venom-injection (Fig. 6C; Additional File 2: Table S6C).

Ontogenetic variation in haemorrhagic potential

Given the ontogenetic variation in the proteomic composition and function of *D. russelii* venoms, the variation in haemorrhagic potential was estimated in the murine model. The mean diameter of the haemorrhagic lesion induced was plotted against various concentrations of venoms tested and simple linear regression was performed. The slopes of the curves obtained for the neonate, juvenile and adult venoms were compared. The slopes were significantly different from one another ($p = 0.0096$). The minimum amount of venom required to induce a 10-mm haemorrhagic lesion was interpolated from these curves. While only 1.23 µg of the adult *D. russelii* venom was sufficient to induce a haemorrhagic lesion of 10 mm, the MHD of the neonate (5 µg/mouse) and juvenile (6.5 µg/mouse) venoms was four to five times higher (Additional file 1: Fig S9 and S10; Additional file 2: Table S7).

In vitro *binding potential of antivenoms*

Indirect enzyme-linked immunosorbent assays (ELISAs) were performed to assess the binding efficacy of various Indian antivenoms against the venoms of adult and younger individuals. Here, the titre values of various antivenoms were calculated by comparing them against the naive horse IgG negative control. These titre values indicate the highest dilution at which the antivenoms exhibit specificity towards the target venom. The negative control cutoff was also used as the baseline the half maximal inhibitory concentration (IC_{50}) estimates. Amongst the four polyvalent antivenom products tested (Additional File 2: Table S4), VINS and Premium Serums performed better against a majority of *D. russelii* and *N. naja* venoms as reported previously [6, 7]. These antivenoms also recognised neonate and adult *D. russelii* venoms similarly, with a titre of 1:12,500 (IC_{50}: 0.6–1 µg/mL; $p < 0.0001$) but exhibited a relatively lower titre towards juvenile venoms [(1:2500); IC_{50}: 4 and 3 µg/mL for VINS and Premium Serums, respectively; $p < 0.0015$; Fig. 7; Additional file 1: Fig S11A]. However, in the case of *N. naja*, antivenoms exhibited slightly

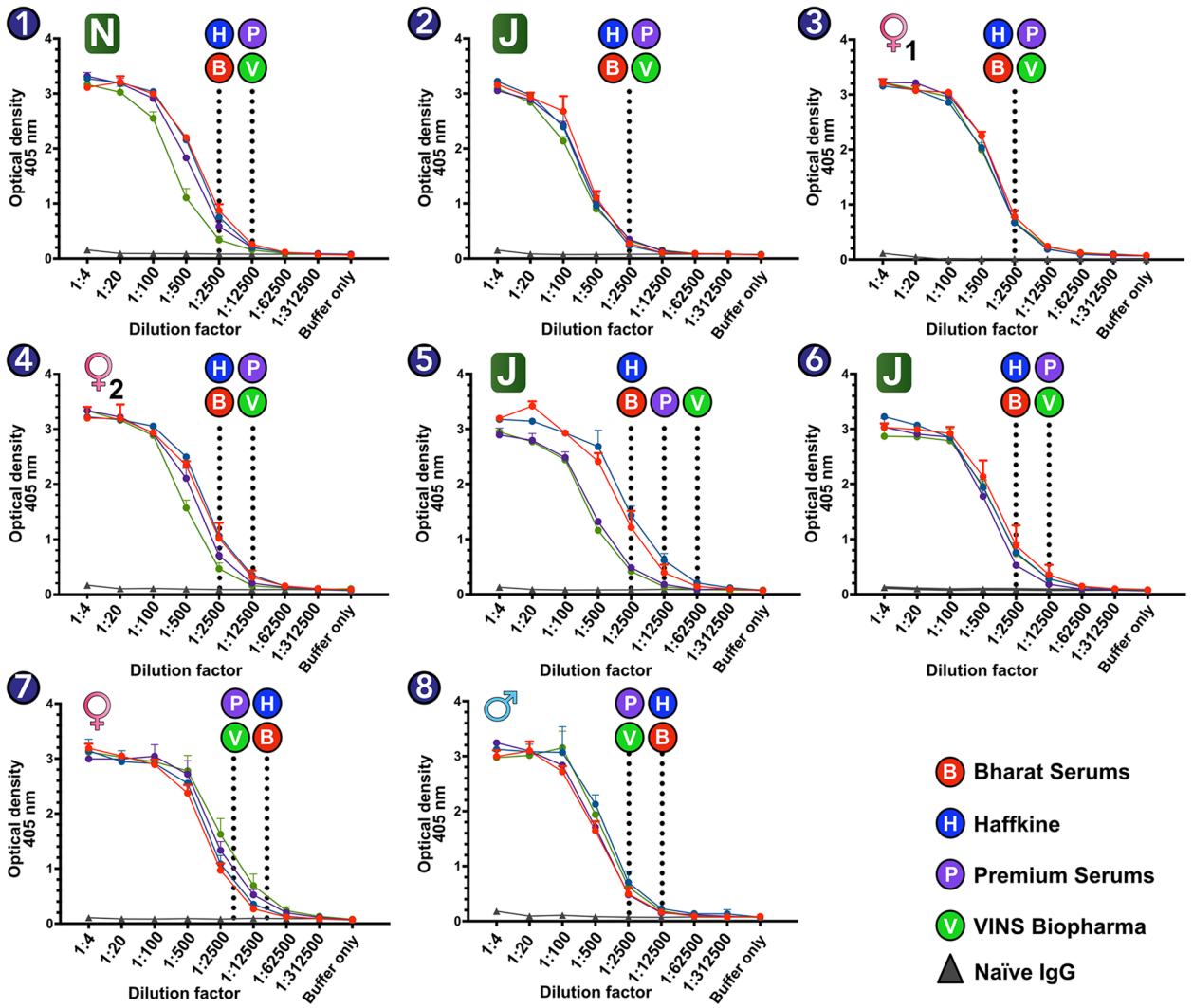

Fig. 7 In vitro binding of antivenoms against the venoms of various ontogenetic stages of *D. russelii* and *N. naja*. Line graphs in this figure depict the in vitro binding potentials of Indian polyvalent antivenoms against the young and adult [1–4] *D. russelii* and [5–8] *N. naja* venoms (replicate $n = 3$). The binding was assessed by plotting absorbance at 405 nm against various dilutions of the antivenom (*x*-axis) in indirect ELISA. Dotted vertical lines indicate the titre values of respective antivenoms calculated using the negative control cutoff. B Bharat Serums and Vaccines Ltd, H Haffkine Bio-Pharmaceutical Corporation Ltd, P Premium Serums & Vaccines Pvt. Ltd, V VINS Bioproducts Ltd. The following symbols represent various developmental stages: N neonate, J juvenile, ♂ unrelated male, ♀ adult mother. The IC_{50} estimates are provided in the Additional file: Fig S11. The supporting data are provided in Additional File 3

higher binding towards the venoms of juveniles and adult females (1:12,500) in comparison to the venom of adult males [a titre of 1:2500, as reported previously [9]]. Though negligible differences were observed in the IC_{50} of various antivenoms towards the venom of *N. naja* juvenile 02 ($p = 0.1240$), the Bharat Serums and Haffkine antivenoms exhibited significantly lower binding towards the juvenile 01 with IC_{50} estimates of 3.5 and 4.2 µg/mL, respectively ($p < 0.0001$; Additional file 1: Fig S11B). Overall, IC_{50} estimates also highlighted that the Premium Serums antivenom exhibited better recognition potential against the *N. naja* and *D. russelii* venoms (Additional file 1: Fig S11). Therefore, based on the titre values and the IC_{50} estimates, the best binding antivenom (Premium Serums) was further downselected for animal protection studies. This downselection was performed with ethical considerations to reduce the total number of mice sacrificed.

In vivo neutralisation potency of polyvalent antivenom

While the in vitro binding assay suggested that Indian antivenoms recognise the venoms of younger and adult individuals with similar efficiency, the in vivo mice toxicity assays revealed the shortcomings of the marketed antivenoms. In line with previous findings, the Premium Serums antivenom, which, despite being one of the best binding antivenoms under in vitro conditions in this study, exhibited lower neutralisation potencies in comparison to the market claim against all tested venoms (Fig. 8). While the marketed neutralisation potency for *D. russelii* and *N. naja* venoms is 0.60 mg/mL, the neutralisation potencies towards the venoms of younger and adult stages of *D. russelii* from Karnataka ranged between 0.319 mg/mL and 0.468 mg/mL (Additional File 2: Table S8A). Similarly, the neutralisation potency of this antivenom against the juvenile (0.221 mg/mL) and adult (0.321 mg/mL) *N. naja* venom was critically lower than the marketed efficiency (Additional File 2: Table S8B).

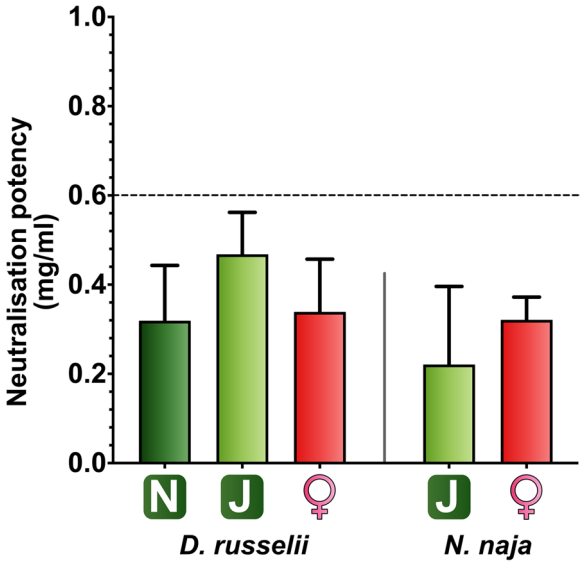

Fig. 8 Neutralisation potencies of commercial polyvalent antivenom against *D. russelii* and *N. naja* venoms from different ontogenetic stages. The bar graphs show the neutralisation potencies of polyvalent antivenom manufactured by Premium Serums. In these graphs, the *x*-axis shows different samples—N neonate, J juvenile 01, ♀ adult mother of *D. russelii* and *N. naja* venoms. The *y*-axis represents neutralisation potency calculated using the LD_{50} of the venoms and the effective dose (ED_{50}) corresponding to that venom in milligrammes per millilitres. The dotted lines parallel to the *x*-axis at 0.6 mg/mL indicate the marketed neutralisation potency of antivenom, and the error bars indicate 95% CI calculated using Probit statistics. Detailed information on the antivenom dose (µl), the survival patterns and ED_{50} values with 95% CI are provided in Additional File 2: Table S8

Discussion

Ontogenetic shift in Russell's viper venoms

Venom is a highly adaptive trait that is crucial for prey capture, defence, competition or a combination thereof [1]. It is, therefore, not surprising that stark inter and intraspecific differences in snake venom composition, activity and toxicity have been reported in various venomous organisms [6–8, 37–41]. Several proteomic and toxinological studies conducted across the geographic distribution of these species have revealed remarkable variations in the abundances of toxins that inflict severe neurotoxicity and coagulopathies [21–26]. In a complete contrast, a recent study has reported the role of certain factors (e.g. dietary specialisation) in promoting the conservation of venom phenotypes across wide geographic distributions [42]. Moreover, various ecological, environmental and life history traits, such as sex, season, and ontogeny, may shape venoms [43–47]. For instance, given the gradual increase in gape size associated with the developmental stage of snakes, variations in diet has been reported [48, 49]. In turn, to facilitate such shifts in diet, ontogenetic shifts in venoms have also been reported [50, 51]. For example, in the case of certain *Crotalus spp.* (e.g. *Crotalus simus simus, C. molossus nigrescens, C. oreganus helleri* and *C. o. oreganus*), the relative abundance of venom toxins shifts from neurotoxic PLA_2s in juveniles to haemotoxic SVMPs in adults to facilitate a corresponding shift in diet from lizards to mammals [52–55]. Thus, developmental stage-specific venom compositions can underpin ontogenetic shifts in diet. However, they remain poorly investigated in snakes around the world.

The influence of ecology and environment in shaping the venoms of Indian snakes, in particular, remains elusive. For instance, while considerable geographical venom variation is well-documented in *D. russelii* and

N. naja [6, 7, 12, 56, 57], the underlying factors responsible for this variation remain unclear. Similarly, ontogenetic shifts in the venoms of Indian snakes have never been investigated. Thus, to address these shortcomings, and to understand the ontogenetic venom variation in Indian snakes, we investigated 194 (from 7 clutches) and 32 (2 from clutches) individuals of *D. russelii* and *N. naja*, respectively. Neonates and juveniles examined in this study were captive-born offsprings of adult females caught in the wild. All adult females and males were caught from the same geographic location (Hunsur, Karnataka, India).

Our findings provide interesting insights into ontogenetic shifts, or lack thereof, in the venoms of *D. russelii* and *N. naja*—India's two clinically most important snake species. Proteomics experiments revealed that the venoms of neonate and juvenile *D. russelii* were predominantly composed of PLA_2 and SVSP. However, the adult venoms transitioned into a more complex repertoire, constituted by CTL, Kunitz and SVMP in nearly equal proportions (Fig. 2; Additional file 2: Tables S2A-C). Enzyme kinetic assays supported these observations, wherein caseinolytic activity, which is largely driven by venom proteases, was recorded only for the venoms of adults (Fig. 4B). Repetition of this assay with EDTA and PMSF inhibitors confirmed that the proteolytic activity of adult venom was driven by SVMP and not by SVSP. While PLA_2s were abundant in the venoms of both younger and adult stages, higher PLA_2 activity was recorded in the former (Fig. 4A; Additional file 2: Tables S2A-C). This could be a result of a relatively higher proportion of catalytically active PLA_2s in the venoms of younger stages. Previous reports have highlighted lower PLA_2 activities in adults of certain populations of *D. russelii* across India [7, 34]. Therefore, it may be interesting to investigate whether adults in these populations lose catalytic PLA_2s due to ontogenetic shifts. Further differences in venom functions were offered by direct haemolysis and haemorrhagic dose experiments. Certain snake venom PLA_2s are known to disrupt the phospholipid bilayer of erythrocytes, resulting in haemolysis [58]. On the contrary, SVMPs are predominantly attributed to the haemorrhagic manifestations observed in viper envenomings [59]. Consistent with the proteomic and functional profile of *D. russelii* venoms, only neonate and juvenile venoms exhibited haemolysis (Fig. 4C), while adults induced haemorrhage at venom concentrations lower than that of younger stages (1.23 µg vs 5–6.5 µg; Additional file 1: Fig S9-S10; Additional File 2: Table S7).

D. russelii venoms are dominated by toxins that inflict intravascular coagulopathy and systemic haemorrhage. SVMPs and SVSPs in *Daboia* venoms activate blood coagulation factor X and factor V, respectively [60, 61]. In addition, SVMPs can induce local and systemic haemorrhage, damage blood vessels and result in profuse internal bleeding and, ultimately, death of bite victims [62]. While these manifestations help in the rapid immobilisation of mammalian prey, human snakebite victims suffer VICC and immutable injuries [15]. Venoms of all developmental stages of *Daboia* exhibited varying levels of fibrinogenolysis, with the neonate and juvenile individuals reducing the plasma fibrinogen concentration significantly more than the adults (30–70 mg/dl vs 160 mg/dl; $p < 0.0001$; Fig. 4E). Such differences could be attributed to the higher proportions of SVSPs in the venoms of younger stages (Fig. 4B; [43]). LAAO, a toxin attributed to platelet aggregation, apoptosis and necrosis in human bite victims [63], was also found in higher proportions in adult venoms (2352–2851 nmol/mg/min) compared to neonates and juveniles (52–147 nmol/mg/min; $p < 0.05$; Fig. 2).

Further evidence of a notable ontogenetic shift in venom phenotypes of *D. russelii* was provided by toxicity assays. When LD_{50} experiments were conducted on rodents, the venoms of *D. russelii* neonates were 2.3 and 2.5 times more potent than their adult mother and juvenile counterparts, respectively. When the venom potency was assessed against lizards, adult *Daboia* did not exhibit toxicity, even up to a dose of 20 mg/kg, whereas neonates and juveniles induced lethality at doses as low as 2–4 mg/kg. We further assessed ontogenetic shifts in toxicities towards insects using crickets (0.5–1 g) as a model system. Here, the venoms of neonates and juveniles did not exhibit toxicity towards insects, even up to doses equivalent to 16 mg/kg (Fig. 6C). In contrast, the venom of adult Daboia eventually killed crickets at a test dose of 6 mg/kg, but the observed toxicity was, perhaps, not intended. Experimental insects injected with these venoms did not exhibit any signs of toxicity but ultimately succumbed to the effects of envenoming 24 h post venom injection. In contrast, the venom of the Indian red scorpion (*Hottentotta tamulus*)—a major insect predator—killed crickets within a minute of injection at concentrations as low as 2.8 mg/kg. These observations suggest that the venoms of *D. russelii* across all developmental stages may not play a role in capturing arthropod prey (Fig. 6C, Additional file 2: Tables S5C and S6C).

In summary, a shift from a higher phospholipolytic neonate and juvenile venoms to a higher proteolytic adult venom was documented in *D. russelii*. Periodic evaluation of venoms of various developmental stages of *D. russelii* in this study reveals that this shift in venom phenotype occurs between 6 and 9 months (Additional file 1: Fig S1 and S4). A similar ontogenetic shift in the venoms of *Crotalus spp.* (Crotalinae) has been reported to occur gradually over a period of 2 years [64]. Interestingly, this

is the first documentation of ontogenetic shift in venom within the Viperinae clade.

A lack of ontogenetic shift in spectacled cobra venoms

In contrast to the considerable ontogenetic shift in venoms of *D. russelii*, developmental stages of *N. naja* were found to produce similarly functional venoms. Except for the marked variation in the proportion of C-3FTx and CRISPs between juvenile and adult venoms (Fig. 3; Additional file 2: Tables S2D-E), the overall composition, biochemical activity and potency of the venom did not significantly change across developmental stages (Figs. 5 and 6). Differences were not observed in the relative abundance of N-3FTx—a major *Naja* toxin superfamily—between the venoms of juveniles and adults (24.4% and 26.5%, respectively; Fig. 3). In vitro binding assays involving *N. naja* venoms and nAChR mimotopes from various animals, including prey and predators of this species, corroborated these findings. Both *N. naja* juvenile and adult venoms exhibited increased binding towards reptilian, amphibian and rodent nAChRs (Fig. 5). This is consistent with field documentation of *N. naja* feeding on these animals [65]. Lower binding was observed towards mongoose, snake and human mimotopes. While the α1 nAChR of the Egyptian mongoose has been previously identified to be resistant to α-neurotoxins [66], the lower binding towards snake receptors could be due to substitutions that prevent autotoxicity [67]. Similarly, relatively weaker binding towards human nAChRs is consistent with the fact that we are neither their prey nor predator. In agreement with the proteomic composition, the venoms of juveniles exhibited higher LAAO activity (775–849 nmol/mg/min) than adults (1762–2389 nmol/mg/min; Fig. 4F). Further, despite the presence of higher amounts of PLA_2s in juveniles (6.3% vs 0.25%; Fig. 3), adults exhibited PLA_2 activity (81–104 nmol/mg/min) that was 2× higher than the former (34–44 nmol/mg/min; $p < 0.05$; Fig. 4G). However, haemolytic activity was not observed in either of these venoms. In toxicity assays, *N. naja* juvenile and adult venoms did not exhibit a marked variation in lethal potencies against mammalian (0.380 mg/kg vs 0.363 mg/kg) and reptilian (0.510 mg/kg vs 1.265 mg/kg) prey. Similarly to the venom of *D. russelii*, *N. naja* venom, too, did not exhibit toxicity towards crickets, suggesting that they do not target arthropods. While ontogenetic shifts were not documented in *N. naja*, inter-individual venom variation was observed in juveniles ($n = 15$; Additional file 1: Fig S2). Notable differences in abundances of LMW toxins, such as 3FTxs (< 15 kDa), were recorded in their SDS-PAGE profiles. Such differences observed in closely related individuals may contribute to considerable intrapopulation venom diversity documented in snakes [8].

Many ways to skin a cat: deployment of broadly effective versus prey-specific toxins across developmental stages

Differing predatory strategies of *D. russelii* and *N. naja* may have shaped their venom compositions and potencies across developmental stages. Spectacled cobra is known to be an opportunistic feeder that actively hunts various prey animals, including lizards, frogs, toads, snakes and rodents [65]. In contrast, Russell's viper is predominantly an ambush predator that probably hunts specific prey at various developmental stages. For instance, we documented caudal luring by neonates in the presence of the common Indian cricket frog (*Minervarya agricola*). During this behaviour, neonates wiggled their tails to mimic worms—a trait that, perhaps, helps them attract prey (Additional file 5). Consistently, *D. russelii* neonate individuals readily accepted frogs in captivity. However, adults have not been documented to exhibit such a behaviour. It is also very clear that gape size limitations prevent neonate *D. russelii* from feeding on larger rodents, further pointing towards a diet shift with age. Consistent with this hypothesis, *D. russelii* was documented to produce distinct venom cocktails across developmental stages that exhibited varying prey specificities. Toxicity experiments revealed that neonate venoms exhibit increased potency towards mice, in comparison to juveniles and adults (Fig. 6A; Additional File 2: Table S5A). However, only neonate and juvenile venoms were lethal to lizards, and adult venoms did not induce lethality even up to a dose of 20 mg/kg (Fig. 6B; Additional File 2: Table S5B).

Several hypotheses could be put forward to explain the observed temporal variation in composition and potency of *D. russelii* venoms. Ontogenetic shifts in venom could relate to the developmental stage-specific changes in the gape size of snakes [48, 49]. Given the limited gape size, the younger stages may be only able to capture smaller reptilian or amphibian prey. Eventually, as adults, with an increased gape size, they could shift to feeding on larger mammals. Field observations in crotaline snakes have also identified a diet shift from ectothermic (arthropod, reptilian or amphibian) to endothermic (mammalian) prey with age, which is underpinned by a corresponding shift in venom profiles [50, 55, 68, 69]. Behavioural observations in this study point to a similar shift in diet from ectotherms (lizards and frogs) to endotherms (rodents) in *D. russelii*. Here, the HMW SVMPs have been implicated in the rapid immobilisation and digestion of large mammalian prey [70, 71], which could explain the shift towards an SVMP-rich venom in adult *D. russelii*. Moreover, an increase in the complexity of venom with age has been previously reported in several species from the Crotalinae clade [43, 47, 72]. Consistent with this, we find that

the venoms of neonate and juvenile *D. russelii* transition into a more complex phenotype in adults, where additional toxin classes, including Kunitz and CTL, are expressed. However, their roles in adult venoms remain unclear and require further investigation.

Another hypothesis that could explain ontogenetic shifts in the composition and potency of *D. russelii* venom pertains to resource optimisation. We find that the venoms of neonate and juvenile *D. russelii* are rich in LMW toxins. While adults produce both LMW and HMW toxins, their LMW components do not appear to be the same as the ones expressed by younger stages (Fig. 2). This, perhaps, suggests that the younger stages produce certain LMW toxins that are responsible for their increased venom potency. Since younger stages also produce relatively smaller amounts of venom, the increased venom potency may compensate for the lack of sufficient yield. Moreover, the expression of highly potent LMW toxins could be metabolically more energy efficient for the newborns, as opposed to the production of large multi-domain SVMPs.

In contrast to stark shifts in *Daboia* venoms, we find that the venoms of *N. naja* are rich in 3FTxs across developmental stages (Fig. 3). Similarly, monocled cobras (*N. kaouthia*) have also been reported to produce 3FTx-rich venoms across their life stages [73]. Structurally and functionally diverse 3FTxs in elapid venoms can exhibit a broad range of prey specificity [74, 75]. In support of this, the results of nAChR binding and toxicity experiments in this study suggest that *N. naja* 3FTxs may facilitate the effective capture of various prey species, including rodents, lizards and amphibians (Figs. 5 and 6). A lack of ontogenetic shift in the venoms of elapids has also been reported in coastal taipans [76]. However, age-associated shifts in biochemical, coagulopathic and toxicity profiles have been documented in others (*N. atra*, *N. nigricolis* and *Pesudonaja spp.*) [77–79].

Studies on ontogenetic shifts in venoms have often invoked paedomorphism—retention of newborn characters into adulthood—to explain similarities between the venoms of younger and adult stages [80, 81]. This theory, first proposed by Walter Garstang in 1922, suggests that competition and predation pressure drive paedomorphism [82]. While contradictory theories have been proposed to explain the evolutionary role of this trait [83], the absence of an ontogenetic shift in *N. naja* venoms may be associated with phylogenetic inertia and not paedomorphy. The expression of diverse 3FTxs in venoms is an ancestral trait observed across the Elapidae clade and, hence, the increased abundance of this toxin family in both juvenile and adult venoms cannot be termed paedomorphy.

The impact of ontogenetic shifts in venom on the effectiveness of snakebite therapeutics

Considerable differences in venom compositions have been shown to reduce the efficiency of marketed antivenoms [39, 81, 84]. Despite the remarkable inter- and intraspecific venom variation, the Indian antivenoms are manufactured by sourcing venom from a point location in southern India and by using a century-old manufacturing strategy. This polyvalent antivenom manufactured against the 'big four' snake venoms has been shown to be ineffective/poorly effective in countering bites from the pan-Indian 'big four' snake populations [6–9]. In addition to geographic variation, studies have also suggested that the ontogenetic shift in venoms may also affect the efficacy of antivenoms [85]. While considerable research has been conducted towards understanding geographic variation in Indian snake venoms and its repercussion on the effectiveness of antivenoms, ontogenetic shifts in venom profiles and their clinical impact have never been documented.

In this study, in vitro binding and in vivo neutralisation potencies of commercial antivenoms from leading Indian manufacturers against the venoms of the developmental stages of *D. russelii* and *N. naja* were assessed. While the in vitro binding assay suggested that these antivenoms recognised the venoms of younger and adult snakes with similarly decent efficiencies (Fig. 7), in vivo neutralisation experiments involving mice revealed their shortcomings (Fig. 8; Additional file 2: Table S8). Our results showed that Premium Serums antivenom, which was one of the best-binding antivenoms under in vitro conditions, exhibited poor neutralisation against the venoms of all developmental stages of both *D. russelii* and *N. naja*. However, whether the observed lack of antivenom efficacy results from ontogenetic shifts in venoms remains unclear. Snake venoms investigated in this study were collected in Hunsur, Karnataka, a high-altitude Deccan Plateau zone, which is starkly different from the coastal regions of Tamil Nadu, where the venoms are sourced for the commercial production antivenoms. Therefore, the observed lack of neutralisation could also stem from the geographic variation in venom. Assessing the neutralisation potencies of Indian antivenoms on the venoms of the developmental stages of snakes from Tamil Nadu will reveal the impact of ontogenetic shifts on snakebite therapeutics. In any case, even when such an impact is documented, understanding the burden of snakebite incidents by younger individuals is imperative for suggesting policy changes for the inclusion of newborn snake venoms in the immunisation mixture.

However, based on these results, it is clear that the biogeographic venom variation plays a greater role in determining the neutralisation potency and, hence, requires

immediate attention. Previous studies have also emphasised the poor performance of Indian antivenoms against the venoms from several *N. naja* populations, including Karnataka [6, 9]. While we note a poor neutralisation potency against *D. russelii* venom from Karnataka, Indian antivenoms have been reported to sufficiently neutralise the lethal effects of *Daboia* venoms of several other populations [7]. The only other exception to this was the northern semi-arid *D. russelii* population [7]. Overall, our findings collectively emphasise the need for the development of region-specific antivenoms that target the venoms of medically important snakes by the region.

Limitations

Due to sampling restrictions by the forest department and insufficient venom yield from the neonate and juvenile Russell's vipers, technical replicates for proteomic analyses, such as RP-HPLC and LC–MS/MS, were not performed. This limitation also hindered our ability to investigate the variations in minor enzymatic components, including 5'-NTD and PDE. While these toxins could contribute to the overall compositional and functional variations between ontogenetic stages, given their limited abundance (< 1%) in the venom proteome, it is unlikely that they play an important ecological or clinical role. This limitation further prevented us from performing comparative nAChR binding assays with *D. russelii* venoms. While we do not expect to find any nAChR-specific toxins in *D. russelii* venom, these assays may shed light on the mild neurotoxic symptoms associated with envenoming from this species in certain parts of India. Additionally, we chose to analyse venoms from a single population in Karnataka to minimise the effects of regional venom variation. While we have documented identical venom profiles for neonates, juveniles and adults from other distant populations, dedicated research can elucidate the extent of ontogenetic venom variation across India. Moreover, our study did not distinguish whether the observed antivenom inefficacy is attributable to regional variation or ontogenetic differences. Future investigations should encompass venom samples from diverse ontogenetic stages collected, particularly from regions where acceptable antivenom efficacies have been demonstrated. These studies are essential to comprehensively understand the ontogenetic and regional variations in venom composition and their implications for antivenom development.

Conclusion

In conclusion, our study provides compelling evidence that ecological and life-history factors significantly influence the composition, function and potency of *D. russelii* and *N. naja* venoms across their developmental stages. While marked ontogenetic shifts in venom profiles were observed in *D. russelii*, the venoms of *N. naja* demonstrated a lack of functional variation across developmental stages. Moreover, the receptor-binding assays revealed that the venoms of *N. naja* exhibit a broad range of specificities towards various prey and predatory animals, thereby explaining the lack of ontogenetic shifts in the venom of this species. These findings unravel the complex interplay between ecological and evolutionary processes that shape venom diversity across different life stages of an individual. Understanding these dynamics not only enhances our knowledge of venom evolution but also has important implications for the development of more effective antivenoms and medical treatments for snakebite victims.

Methods

Venoms evaluated in this study

Venoms of *N. naja* and *D. russelii* individuals of various developmental stages, including neonates (< 30 days), juveniles (between 1 to 12 months) and mature individuals (> 36 months), were sampled with permission from the state forest department of Karnataka (PCCF(WL)/E2/CR-06/2018–19 and PCCF(W1)/C1(C3)/CR-09/2017–18); 226 individuals from 9 clutches were examined. Of these, 194 individuals belonged to seven clutches of *D. russelii*, and 32 belonged to two clutches of *N. naja*. Venom was sourced every 3 months from *N. naja* and *D. russelii* individuals to track ontogenetic changes across time. Freshly collected venoms were flash-frozen in liquid nitrogen, lyophilised and stored at − 80° C. A detailed list of venom samples analysed in this study is provided in Additional file 2: Tables S1A-B. Adult male and female snakes rescued from the Hunsur City in the Mysore district of Karnataka were housed in the same locality, and their venoms were collected periodically. Gravid females gave birth to the neonates used in the study under captive conditions. This strategy was adopted to negate the effect of intrapopulation venom variation on our findings. As venom could exhibit significant intrapopulation venom variation, even at shorter geographic scales [8], the distribution of the samples was restricted to a few kilometres around the housing site. Throughout the experimental time, all snakes were raised on a rodent diet.

Reversed-phase high-performance liquid chromatography (RP-HPLC)

Snake venoms were fractionated on a Shimadzu LC-20AD series HPLC system (Kyoto, Japan), following a modified version of the previously published protocol [12, 86]; 1 mg of venom diluted in water was injected into a reversed-phase C18 Shim-Pack GIST column [4.6 × 250 mm, 5 µm particle size and 100 Å pore size

(Shimadzu, Japan)], previously equilibrated with 95% buffer A [0.1% trifluoroacetic acid (TFA) in water (v/v)] and 5% buffer B [0.1% TFA in acetonitrile (v/v)]. Venom fractions were eluted at a steady flow rate of 1 mL/min under a gradient of buffer A (0.1% TFA in HPLC grade water), buffer B (0.1% TFA in acetonitrile) and isocratic (5% buffer B) for 5 min, followed by 5–15% buffer B for 10 min, 15–45% buffer B for 60 min and 45–70% buffer B for 10 min and held at 70% buffer B for 9 min, followed by 70–98% buffer B for 6 min and again held at 98% buffer B for 5 min and completed with 5% buffer B for 5 min. The column was equilibrated at 5% buffer B for 10 min, completing a total run time of 120 min. Fractions were collected separately by monitoring the absorbance peaks at 215 nm, and the areas under the peaks were estimated to calculate their relative abundances.

Protein estimation and gel electrophoresis

The above fractions were concentrated in a vacuum centrifuge (Thermofisher Scientific, USA), followed by resuspension in ultrapure water. These fractions were subjected to 12.5% SDS-PAGE under reducing conditions at a constant voltage of 80 V [87]. Following this, the gels were stained overnight with Coomassie Brilliant Blue R-250 (Sisco Research Laboratories Pvt. Ltd, India) and visualised using an iBright CL1000 gel documentation system (Thermo Fisher Scientific, MA, USA). The densitometry analysis of individual bands was then performed using the ImageJ software [88] and the bands were excised for mass spectrometric analyses.

In-solution and in-gel trypsin digestion

A combined analysis strategy was adopted for mass spectrometry, wherein RP-HPLC fractions with higher peak area were subjected to reducing SDS-PAGE and smaller peaks that could not be visualised on the gel were directly subjected to in-solution digestion. The excised gel bands were destained using 30% acetonitrile in 50 mM ammonium bicarbonate buffer. The gel pieces were dehydrated using 100% acetonitrile, followed by reduction using 10 mM dithiothreitol (DTT) at 56 °C for 45 min and alkylation using 55 mM iodoacetamide for 35 min at room temperature. The samples were then digested using sequencing-grade trypsin and incubated overnight at 37 °C. The following day, the supernatant was collected and desalted in a Pierce C18 spin column (Thermofisher Scientific, USA) following the manufacturer's protocol before being subjected to mass spectrometric analyses. Similarly, for in-solution digestion, fractions were reduced and alkylated using DTT (100 mM) and iodoacetamide (100 mM), respectively, followed by tryptic digestion.

Liquid chromatography-tandem mass spectrometry (LC–MS/MS)

The digested peptides were subjected to nano-liquid chromatography (nano-LC) and electrospray ionisation tandem mass spectrometry (ESI–MS/MS). The samples were injected into a PepMap C18 nano-LC column (50 cm × 75 µm, 2 µm particle size and 100 Å pore size) mounted on the Thermo EASY nLC Ultimate 3000 series system (Thermo Fisher Scientific, MA, USA), following a gradient elution of buffer A (0.1% formic acid in MS grade water) and buffer B (0.1% formic acid in 80% acetonitrile) at a constant flow rate of 250 nL/min for 90 min. An 8–35% gradient of buffer B was used over the first 70 min for elution, followed by 35–95% over the next 5 min, and finally 95% for the last 15 min. Subsequently, the fractions from the nano-LC were injected into a Thermo Orbitrap Fusion Mass Spectrometer (Thermo Fisher Scientific, MA, USA). The following protocol was adopted to perform the MS scans: scan range (m/z) of 300–2000 with a resolution of 120,000 and maximum injection time of 100 ms. To perform the precursor (MS) and fragment (MS/MS) scans, an orbitrap detector with high collision dissociation (HCD) fragmentation (30%) was used with the following parameters: scan range (m/z) of 110–2000 and maximum injection time of 50 ms [89].

Raw MS/MS spectra were searched against the National Center for Biotechnology Information non-redundant (NCBI-NR) Serpentes database (taxid: 8570; with 549,650 entries as of September 2023) to identify toxins that constitute the venom fractions. The search was performed in PEAKS Studio X Plus software (Bioinformatics Solutions Inc., ON, Canada) by setting parent and fragment mass error tolerance limits to 10 ppm and 0.6 Da, respectively. A 'monoisotopic' precursor ion search type and semispecific trypsin digestion were specified as parameters. Fixed and variable modifications were set as carbamidomethylation (+57.02) and oxidation (+14.99), respectively. The false discovery rate (FDR) was set to 0.1%, and PEAKS Studio automatically determined the corresponding −10lgP cutoff value. Hits with at least one unique matching peptide were considered for protein identification, and redundant hits from each protein family were manually removed.

The proportions of toxins in the venom were determined by implementing a multipronged normalisation strategy [12, 89–92]. First, the area under the curve of spectral intensities of a toxin hit (AUC_t) was normalised within the fraction using the formula below.

$$(\mathrm{AUC})_{\mathrm{MS}} = \frac{\mathrm{AUC}_t}{\sum_{t=1}^{N} (\mathrm{AUC})_t}$$

Here, AUC_{MS} represents the normalised AUC_t, while '*t*' represents toxins in a given fraction and *N* denotes the total number of toxins in that fraction.

To calculate the proportion of the *i*th toxin (T_i) in the venom, the obtained AUC_{MS} was further normalised by multiplying with the relative RP-HPLC area (AUC_{HPLC}) of the respective fraction and the density (*D*) of the SDS-PAGE band.

$$T_i = \sum_{f=1}^{N} (\mathrm{AUC_{HPLC}} \times D \times \mathrm{AUC_{MS}})_f)$$

Here, '*N*' denotes the total number of fractions.

The toxins were further categorised into their respective families, and the relative abundance (%) of each family was calculated by summing up the proportions (T_i) of all the toxins within that family. Mass spectrometry data is deposited to the ProteomeXchange Consortium via the PRIDE partner repository with data identifiers PXD046781 [93]. The list of toxins identified through tandem MS and their relative proportions are tabulated in Additional file 2: Tables S2A-E.

Biochemical and pharmacological analyses

Differences in biochemical and pharmacological activities of venoms of mother snakes and their offspring were evaluated using various assays, including PLA_2, SVSP, SVMP, LAAO and fibrinogenolysis. All concentrations of venoms and reagents used in the assays were based on dose–response experiments performed as previously described.

Colourimetric PLA2 assay

A chromogenic lipid substrate, 4-nitro-3-[octanoyloxy] benzoic acid (NOB; Enzo Life Sciences, New York, NY, USA), was used to determine the PLA_2 activity of venoms. A known amount of venom (5 µg) was incubated at 37° C for 40 min with 500 mM substrate in a total reaction volume of 200 µl made up using the NOB buffer (10 mM Tris–HCl, 10 mM $CaCl_2$, 100 mM NaCl, pH 7.8). The assay kinetics was recorded by measuring the absorbance at 425 nm every 10 min using an Epoch 2 microplate spectrophotometer (BioTek Instruments, Inc., USA). Further, a standard curve was plotted with 4 M NaOH and varying concentrations of the NOB substrate (4 to 130 nmol) following an identical protocol. The amount of the phospholipid substrate (nmol) cleaved per minute per mg of the venom was calculated from the standard curve [94, 95].

LAAO assay

The LAAO activity of venoms was evaluated using a modified colourimetric assay described previously [95, 96]; 200 µl of the L-leucine substrate solution (600 µl of 5 mM L-leucine, 120 µl of 5 IU/mL horseradish peroxidase, 1200 µl of 2 mM o-phenylenediamine dihydrochloride, 6000 µl of 50 nM Tris–HCl buffer at pH 8) and 0.5 µg of the crude venom were preincubated separately at 37 °C for 10 min. Following this, the venom and substrate solution was mixed and incubated at 37 °C. After 10 min, the reaction was terminated by the addition of 2 M H_2SO_4 solution and the amount of H_2O_2 released was quantified by measuring the absorbance of the solution at 492 nm using an Epoch 2 microplate spectrophotometer (BioTek Instruments, Inc., USA). A standard curve of H_2O_2 with concentrations between 0 and 4.895 nmol/min was constructed using a similar protocol. The LAAO activity of venom samples was estimated as the nmol of H_2O_2 released per minute per mg of venom using this standard curve.

Protease assay

The snake venom protease activity was assessed using an azocasein substrate following a protocol described earlier [97]. To assess the relative contribution of SVMP and SVSP to the overall proteolytic activity, 10 µg of the crude venom was incubated at 37 °C for 15 min with 0.1 M EDTA or PMSF, respectively [98, 99]. Venoms were also incubated in the presence and absence of both inhibitors as control. Following treatment with the inhibitor, samples were incubated with the azocasein substrate (400 µg) at 37 °C for 90 min. After stopping the reaction with trichloroacetic acid (200 µl), the reaction mixture was centrifuged at 1000×*g* for 5 min to remove the cleaved products. Equal volumes of 0.5 M NaOH were added to the supernatant, and the absorbance was measured at 440 nm in an Epoch 2 microplate spectrophotometer (BioTek Instruments, Inc., USA). The relative protease activity of venoms was calculated against a purified bovine pancreatic protease (Sigma-Aldrich, USA).

Haemolytic assay

The direct haemolytic effect was assessed by treating known concentrations of venoms (5 to 40 µg) with red blood cells (RBCs) isolated from healthy human volunteers. Briefly, blood was collected in a 3.2% sodium citrate tube and centrifuged at 3000×*g* for 5 min at 4 °C. Post the separation of the platelet-poor plasma (PPP), RBCs were washed with PBS to remove residual proteins. Following this, venoms were added to the RBC suspension in a ratio of 1:9 and incubated at 37 °C for 24 h. The amount of heme released during the breakdown of RBCs was then monitored by measuring the absorbance of the supernatant at 540 nm [100]. The relative haemolytic activity was calculated using Triton X as a positive control.

Fibrinogen quantification assay

The ability of venoms to reduce the total active fibrinogen content in plasma was assessed through von Clauss fibrinogen assay using a commercially available Fibroquant kit (Tulip Diagnostics, Goa, India). A standard curve was constructed using various dilutions of a fibrinogen calibrator solution in Owren's buffer (Undiluted, 1:5 and 1:10 v/v) following the manufacturer's protocol. The time to form the first fibrin clot was plotted against the total fibrinogen concentration in mg/dl. PPP separated from human blood, collected after the removal of RBCs, was diluted in Owren's buffer (1:10 v/v), and 40 µg of venom was added. The mixture was incubated at 37 °C for 180 s. In parallel, bovine thrombin was activated by separately incubating at 37 °C for 60 s. The time taken for fibrin clot formation following the addition of thrombin to the plasma–venom mixture was measured using the optomechanical principle in a Hemostar XF 2.0 (Tulip Diagnostics, Goa, India).

Fibrinogenolytic assay

The fibrinogenolytic activity of venom was electrophoretically assessed using a previously described methodology [101]. A predefined quantity of venom (1.5 µg) was dissolved in phosphate-buffered saline (PBS; pH: 7.4) and incubated with 1 µl of SVMP- (0.1 M EDTA) and/or SVSP- (0.04 M PMSF) inhibitors at 37 °C for 15 min [102]. Following this, 15 µg of human fibrinogen (Sigma-Aldrich, USA) was added to the treatment groups and the samples were further incubated at 37 °C for 60 min. After stopping the reaction by the addition of equal volumes of sample loading buffer (1 M Tris–HCl, pH 6.8; 50% Glycerol; 0.5% Bromophenol blue; 10% SDS; and 20% β-mercaptoethanol) and heat treatment at 70 °C for 10 min, samples were subjected to a 15% SDS-PAGE. Densitometric analyses were performed using the ImageJ software to assess the cleavage pattern of the three fibrinogen subunits in the treatment groups compared to the untreated control [88].

Nicotinic acetylcholine receptor specificity

The binding kinetics between cobra venom neurotoxins and nAChRs from various prey/predatory organisms were determined using a Biolayer interferometry (BLI) assay in an Octet Red 96 system (ForteBio, Sartorius, Fremont, CA). The amino acid sequence of this 14 residue-long orthosteric binding site of the α-neuroreceptor was obtained from the Uniprot database (Additional File 2: Table S3) and chemically synthesised by Genpro Biotech (Uttar Pradesh, India). Following previously described protocols [103], the mimotopes were synthesised with two molecules of aminohexanoic acid (Ahx) spacers to separate the amino acid sequence from biotin to avoid steric hindrance. Additionally, disulphide bridges were replaced with Ser-Ser to prevent thiol oxidation without affecting the binding efficiency, as demonstrated previously [104, 105]. Lyophilised stocks of the mimotopes were reconstituted in 100% dimethyl sulfoxide (DMSO) and stored at − 80 °C until use. A final working concentration of 1 µg/mL was prepared by diluting the mimotope stock in the running buffer [1 × Dulbecco's phosphate-buffered saline (DPBS) with 1% BSA and 0.05% Tween-20]. Similarly, the reconstituted venom samples were also diluted to a concentration of 25 µg/mL in the running buffer. The assay was performed with 5 µg of venom and 0.2 µg of the mimotope solution per well in a black 96-well microtiter plate.

The streptavidin sensors were hydrated in the running buffer for 30 min before the beginning of the experiment. The following data acquisition programme was set up: 60 s baseline, 600 s loading, 100 s baseline, 400 s association and 200 s dissociation. The running buffer and mimotopes were introduced, following the loading of venoms onto the sensor tip. A running buffer control was included along with each venom sample, and the thickness of the molecular layer or wavelength shift (in nm) was recorded and plotted against time (sec) to visualise the association and dissociation kinetics. The exported data was inter-step corrected by aligning the baseline to the *Y*-axis of the initial baseline step, and the dissociation curve was aligned with the association curve. The high-frequency noise in the data was also removed using the Savitsky–Golay filter. The area under the association and dissociation curve was calculated using GraphPad Prism 8.4.3 (GraphPad Software Inc., La Jolla, CA, USA).

In vivo venom toxicity and morbidity

The variation and similarities in the venom lethalities and haemorrhage-inducing potencies were evaluated in the mouse model.

The median lethal dose

Variation in lethal potencies of venoms across developmental stages was determined by estimating the median lethal dose using the mouse model (*Mus musculus*) of envenoming [106]. The LD_{50} value indicates the minimum amount of venom required to kill 50% of the test population injected with venom. Five graded concentrations of crude venoms were intravenously injected into the tail vein of five male CD-1 mice (18–22 g) per venom dose group. Subsequently, the mortality in each group was recorded post a 24-h time window. These values were plotted against venom doses to estimate the LD_{50} using Probit statistics [107].

The lethal potencies of venoms against house geckos (*Hemidactylus frenatus*) and house crickets (*Acheta*

domesticus) were determined by intraperitoneally injecting five graded concentrations of venoms into three individuals per dose group as described previously [108]. Venom doses ranging from 1 to 20 mg/kg and 2 to 16 mg/kg were injected into geckos and crickets, respectively. The mortalities were recorded over a period of 24 h. Scorpion venoms were tested against crickets as a positive control. Geckos and crickets injected with 0.9% physiological saline and Ringer's insect saline [109] served as a negative control, respectively.

The minimum haemorrhagic dose (MHD)

The minimum haemorrhagic dose of a venom (MHD) is defined as the amount of venom (in µg) which induces a 10-mm haemorrhagic lesion within 2–3 h of intradermal injection in mice [106]. Five graded venom concentrations were dissolved in normal saline (50 µl) and intradermally injected into each mouse. Five male CD-1 mice (18–22 gm) were injected per concentration to obtain a statistically significant value. After 3 h, the mice were humanely euthanised, and the dorsal skin patch was examined to assess the diameter of the haemorrhagic lesion. Measurements of lesion diameter from individual mice were taken using a vernier calliper to obtain the mean diameter at a given concentration. Subsequently, a dosage at which the lesion diameter is 10 mm was considered the MHD of a given venom by interpolating from a simple linear equation. A group of five mice injected with normal saline served as a negative control.

In vitro *and* in vivo *antivenomics*

Enzyme-linked immunosorbent assay

The in vitro venom recognition potential of commercial antivenoms was evaluated using the previously described ELISA protocol [110]. The details of the antivenoms tested are mentioned in Additional File 2: Table S4. Venom samples (100 ng) diluted in a carbonate buffer (pH 9.6) were coated onto 96-well plates and incubated overnight at 4° C. Following a brief washing step (six times) with Tris-buffered saline with 1% Tween 20 (TBST) to remove the unbound proteins, a blocking buffer (5% skimmed milk in TBST) was added to reduce non-specific binding. After incubating the plate for 3 h at room temperature, the plate was rewashed, and serially diluted antivenoms (Premium Serums, VINS Bioproducts, Bharat Serums, and Haffkine Biopharma at 1 mg/mL initial concentration) were added. The plate was subsequently incubated overnight at 4 °C. This step was followed by brief washing and incubation with horseradish peroxidase (HRP)-conjugated rabbit anti-horse secondary antibody (Sigma-Aldrich, USA) diluted in PBS (1:1000) for 2 h. Post incubation, ABTS (2,2'-azinobis (3-ethylbenzothiazoline-6-sulfonic acid)) substrate solution (Sigma-Aldrich, USA) was added. The absorbance values were measured at a wavelength of 405 nm for 40 min in the Epoch 2 microplate reader and plotted against the antivenom dilutions to determine the antibody titres. Immunoglobulin (IgG) from unimmunised (naive) horses (Biorad) was used for determining the extent of non-specific binding exhibited by equine antibodies [5]. The non-specific binding cut-off was calculated as the mean absorbance of the negative control plus two times the standard deviation. Further, the titre for a particular antivenom was considered as the first dilution where the binding (mean absorbance) was above this cut-off value. The binding efficacy of the antivenom is considered better if the titre (or dilution) is higher. Additionally, the IC_{50} concentrations of various antivenoms were also calculated. The non-specific binding cut-off calculated above was considered as the baseline value for calculating the IC_{50} and the 95% CI.

Median effective dose (ED50)

In vivo neutralisation potency of commercial antivenoms was determined by estimating their ED_{50} values using WHO-recommended preclinical assays [106]. These values indicate the minimum volume of the reconstituted antivenom required to protect 50% of mice injected with a $5\times LD_{50}$ challenge dose of venom. Venoms were pre-incubated with various concentrations of antivenom at 37 °C for 30 min. These mixtures with five graded concentrations of antivenoms were intravenously injected into the tail vein of five male CD-1 mice (18–22 g) per dose group. Subsequently, the mortality and survival rate in each group were recorded post a 24-h time window. These values were plotted against antivenom doses to estimate the ED_{50} and 95% CI using Probit statistics [107]. ED_{50} values were transformed to neutralisation potency after considering the venom dosage, based on the following Eq. [74]. Here, n represents the number of LD_{50} used as the challenge dose.

$$\text{Neutralisation potency}\left(\frac{\text{mg}}{\text{mL}}\right)=\frac{(n-1)\times \text{LD}_{50}\text{ofvenom}\left(\frac{\text{mg}}{\text{mouse}}\right)}{\text{ED}_{50}\text{ofantivenom(mL)}}$$

Statistical analysis

Statistical comparisons in various biochemical assays were performed using one-way ANOVA with Tukey's and Dunnett's multiple comparison tests. Probit statistics were used for LD_{50} and ED_{50} experiments to calculate the median doses and the 95% CI. Simple linear regression curve fitting was performed for the MHD experiment, and the doses were interpolated from the equation. Two-way ANOVA was used to compare the area under the association and dissociation curves in BLI. For calculating the in vitro IC_{50} values of antivenoms and assessing

if the values are significantly different between various antivenoms, the non-linear regression curve fitting and the sum of squares F test were used. All statistical analyses were performed in GraphPad Prism (GraphPad Software 8.0, San Diego, California USA, www.graphpad.com).

Abbreviations

ACE	Acetylcholinesterase
Ahx	Aminohexanoic acid
ANOVA	Analysis of variation
AUC	Area under the curve
AUC_{HPLC}	HPLC peak area
AUC_{MS}	Normalised spectral intensity of toxin T
AUC_{T}	Spectral intensity of toxin T
BLI	Biolayer interferometry
C-3FTx	Cytotoxic three finger toxins
CI	Confidence intervals
CRISP	Cysteine-rich secretory proteins
CTL	C-type lectins
CVF	Cobra venom factor
DMSO	Dimethyl sulfoxide
DTT	Dithiothreitol
ED_{50}	Median effective dose
EDTA	Ethylenediaminetetraacetic acid
ELISA	Enyzme-linked immunosorbent assay
ESI-MS	Electrospray ionisation mass spectrometry
FDR	False discovery rate
HCD	High collision dissociation
HMW	High molecular weight
IC_{50}	Half-maximal inhibitory concentration
IgG	Immunoglobulin G
Kunitz	Kunitz-type serine protease inhibitors
LAAO	L-amino acid oxidase
LD_{50}	Median lethal dose
LMW	Low molecular weight
MHD	Minimum haemorrhagic dose
N-3FTx	Neurotoxic three finger toxins
nAChR	Nicotinic acetylcholine receptor
NCBI	National Center for Biotechnology Information
NGF	Nerve growth factor
NOB	4-Nitro-3-[octanoyloxy] benzoic acid
PBS	Phosphate-buffered saline
PLA_2	Phospholipase A_2
PMSF	Phenylmethylsulfonyl fluoride
PPP	Platelet-poor plasma
RBC	Red blood cells
RP-HPLC	Reverse phase high pressure liquid chromatography
SDS-PAGE	Sodium dodecyl sulphate polyacrylamide gel electrophoresis
SVMP	Snake venom metalloproteinases
SVSP	Snake venom serine proteinases
TBST	Tris-buffered saline with 1% Tween 20
TFA	Trifluoroacetic acid
VEGF	Vascular endothelial growth factor
VICC	Venom-induced consumption coagulopathy
WHO	World Health Organization

Supplementary Information

The online version contains supplementary material available at https://doi.org/10.1186/s12915-024-01960-8.

Additional file 1: Supplementary_figure. Fig S1. SDS-PAGE profiles of *D. russelii* venoms across developmental stages. The figure depicts venom profiles of neonatesand juvenilescompared to their adult mother. Further details of these venoms are provided in Additional file 2: Table S1. Fig S2. SDS-PAGE profiles of *N. naja* venoms across developmental stages. The figure depicts venom profiles of neonatesand juvenilescompared to their adult mother. Further details of these venoms are provided in Additional file 2: Table S2. Fig S3. SDS-PAGE profiles of venoms from males and females of *D. russelii* and *N. naja*. The figure depicts venom profiles from unrelated adult females and males from Hunsur, Karnataka of *D. russelii* and *N. naja*. Fig S4. RP-HPLC chromatograms for *N. naja* and *D. russelii*. The figure depicts the overlay of three replicatesof venoms from the same individuals of *N. naja* and *D. russelii*. Fig S5. SDS-PAGE profiles of RP-HPLC fractions performed for *D. russelii* and *N. naja* venoms across developmental stages. Fig S6. Enzymatic activities of *D. russelii* venoms across developmental stages. The figure depicts the PLA_2 and protease activities of venoms of *D. russelii* neonates, juvenilesand adult females. The assays were performed in triplicates. The supporting data are provided in Additional file 3. Fig S7. Fibrinogenolytic activities of *Naja naja* and *Daboia russelii* venoms across developmental stages. The figure demonstrates the fibrinogen degradation profilesof the venoms from Adult female, Adult male, Neonate and Juvenile. The lanes indicate various treatment groups- HF: human fibrinogen; 1: Venom + HF; 2: Venom + EDTA + HF; 3: Venom + PMSF + HF; 4: Venom + EDTA + PMSF + HF. Fig S8. Area under the curve comparisons of *N. naja* venom and nAChRs binding kinetics. The figure depicts the area under the curve of *N. naja* venom and nAChRs binding kinetics measured using biolayer interferometry. The AUCs were plotted separately for the association and dissociation kinetics. Fig S9. MHD of *D. russelii* venoms across developmental stages. The figure depicts the dose-dependent increase in the diameter of *D. russelii* venom-induced haemorrhage in mice. The minimum amount of venom required to induce a haemorrhagic lesion of 10 mm diameteris provided for each sample. Linear regression was performed, and the line equation obtainedwas used to interpolate xat y = 10. Fig S10. The haemorrhagic potential of *D. russelii* venoms across developmental stages. The figure depicts the dose-dependent increase in the diameter of *D. russelii* venom-induced haemorrhage in mice. Fig S11. IC_{50} of antivenoms against *D. russelii* and *N. naja* venoms. The figure depicts the IC_{50} of antivenoms against *D. russelii* and *N. naja* venoms, which were calculated from the *in vitro* ELISA experiments.

Additional file 2: Supplementary_Tables. Table S1A: Details of *D. russelii* venom samples investigated in this study. The table depicts the sample IDs, the ontogenetic stage, the number of individual snakes pooled in a sample, the parentage of the individuals included in a sample, their gender and the protein concentrations of all the *D. russelii* venoms assessed in the study. Table S1B: Details of *N. naja* venom samples investigated in this study. The table depicts the sample IDs, the ontogenetic stage, the number of individual snakes pooled in a sample, the parentage of the individuals included in a sample, their gender and the protein concentrations of all the *N. naja* venoms assessed in the study. Table S2A: Proteomic data for *D. russelii* adult venom. Assignment of peptides sequenced from MS/MS spectra using Serpentes NCBI databasein PEAKS X. The relative abundance of each toxin was estimated using methods described in the Methodology section. 10logP is the matching score given by the PEAKS Algorithm, and m/z is the mass-to-charge ratio of the peptides. Table S2B: Proteomic data for *D. russelii* juvenile venom. Assignment of peptides sequenced from MS/MS spectra using Serpentes NCBI databasein PEAKS X. The relative abundance of each toxin was estimated using methods described in the Methodology section. 10logP is the matching score given by the PEAKS Algorithm, and m/z is the mass-to-charge ratio of the peptides. Table S2C: Proteomic data for *D. russelii* neonate venom. Assignment of peptides sequenced from MS/MS spectra using Serpentes NCBI databasein PEAKS X. The relative abundance of each toxin was estimated using methods described in the Methodology section. 10logP is the matching score given by the PEAKS Algorithm, and m/z is the mass-to-charge ratio of the peptides. Table S2D: Proteomic data for *N. naja* adult venom. Assignment of peptides sequenced from MS/MS spectra using Serpentes NCBI databasein PEAKS X. The relative abundance of each toxin was estimated using methods described in the Methodology section. 10logP is the matching score given by the PEAKS Algorithm, and m/z is the mass-to-charge ratio of the peptides. Table S2E: Proteomic data for *N. naja* juvenile venom. Assignment of peptides sequenced from MS/MS spectra using Serpentes NCBI databasein PEAKS X. The relative abundance of each toxin was estimated using methods described in the Methodology section. 10logP is the matching score given by the PEAKS Algorithm, and m/z is the mass-to-charge ratio of the peptides. Table S3: Details of nAChR

mimetopes synthesised in the study. The table depicts the UniProt IDs and the orthosteric binding site sequences of nAChRs from various prey and predator species of *N. naja*. Table S4. Details of antivenom samples investigated in this study. It includes information on batch numbers, manufacture and expiry dates and protein concentrations. Table S5A. Toxicities of *D. russelii* venoms against mice. The table includes venom dose for each mice group, number of survivors and LD_{50}. Table S5B. Toxicities of *D. russelii* venoms against geckos. The table includes venom dose for each mice group, number of survivors and LD_{50}. Table S5C. Toxicities of *D. russelii* venoms against crickets. The table includes venom dose for each mice group, number of survivors and LD_{50}. Table S6A. Toxicities of *N. naja* venoms against mice. The table includes venom dose for each mice group, number of survivors and LD_{50}. Table S6B. Toxicities of *N. naja* venoms against geckos. The table includes venom dose for each mice group, number of survivors and LD_{50}. Table S6C. Toxicities of *N. naja* venoms against crickets. The table includes venom dose for each mice group, number of survivors and LD_{50}. Table S7. Haemorrhagic potential of *D. russelii* venoms. The table outlines the venom dosages, the diameters of the haemorrhagic lesion observed in each mouse injected with the respective venom dose, the mean diameter of the lesion at a given concentration and the minimum haemorrhagic dose. Table S8A. Neutralisation potency of commercial antivenom against *D. russelii* venoms. These tables contain the commercial antivenom dosages, the respective survival patterns, median effective doses and neutralisation potencies. Table S8B. Neutralisation potency of commercial antivenom against *N. naja* venoms. These tables contain the commercial antivenom dosages, the respective survival patterns, median effective doses and neutralisation potencies.

Additional file 3. Raw data for biochemical assays, BLI and ELISA.

Additional file 4. Proteomic analyses of *D. russelii* and *N. naja* venoms.

Additional file 5. Documentation of caudal luring behaviour by neonate *D. russelii*

Acknowledgements
The authors are thankful to the Forest Department of Karnataka for the venom sampling permits, to Mr. Prasad (IISc, Bangalore) and Mr. Anurag (IISc, Bangalore) for the assistance with collection of geckos and to Mr. Muralidhar Naik (IISc, Bangalore) for the assistance with proteomics. We also are thankful to Mr. Navaneel Sarangi (IISc, Bangalore) for the assistance with the functional assay results in Additional file 1: Fig S6.

Authors' contributions
K.S. conceptualised the idea. R.R.S.L. and K.S. designed the study. R.R.S.L., G.M. and K.S collected the venom samples. R.R.S.L, S.B. and K.S. performed the proteomic experiments. R.R.S.L. performed the functional assays. R.R.S.L. and S.K. performed the animal experiments. R.R.S.L., S.B. and K.S. analysed the data. K.S. prepared the main figures. R.R.S.L, S.B, S.K, G.M. and K.S prepared the additional information. K.S acquired the funding. R.R.S.L, S.B. and K.S wrote the original draft of the manuscript. All authors reviewed and edited the manuscript. All authors read and approved the final manuscript.

Funding
KS was supported by the Wellcome Trust DBT India Alliance Fellowship (IA/I/19/2/504647). RRSL was supported by the Prime Minister's Research Fellowship (PMRF) from the Ministry of Human Resource Development (MHRD).

Availability of data and materials
The raw proteomics data generated for this study can be found in PRIDE Database (Accession No: PXD046781). All data generated or analysed during this study are included in this published article, its additional information files and publicly available repositories.

Declarations

Ethics approval and consent to participate
Ethical clearance to evaluate the effects of *Naja* and *Daboia* venoms on various animal models was granted by the Institutional Animal Ethics Committee (IAEC), Indian Institute of Science (IISc), Bangalore (CAF/Ethics/794/2020). All experiments involving animals have been performed following the guidelines of the Committee for Control and Supervision of Experiments on Animals (CCSEA), Government of India. Coagulopathic and haemotoxic effects of venoms on human blood were assessed with permission from the Institute Human Ethical Committee (IHEC No: 18/20201216).
Blood was collected from healthy volunteers after obtaining informed consent.

Consent for publication
Not applicable.

Competing interests
The authors declare that the research was conducted in the absence of any commercial or financial relationships that could be construed as a potential conflict of interest.

Received: 30 January 2024 Accepted: 15 July 2024
Published online: 29 July 2024

References

1. Casewell NR, Jackson TN, Laustsen AH, Sunagar K. Causes and consequences of snake venom variation. Trends Pharmacol Sci. 2020;41(8):570–81.
2. Sunagar K, Morgenstern D, Reitzel AM, Moran Y. Ecological venomics: how genomics, transcriptomics and proteomics can shed new light on the ecology and evolution of venom. J Proteomics. 2016;135:62–72.
3. Jackson TN, Jouanne H, Vidal N. Snake venom in context: neglected clades and concepts. Front Ecol Evol. 2019;7:332.
4. Suraweera W, Warrell D, Whitaker R, Menon G, Rodrigues R, Fu SH, et al. Trends in snakebite deaths in India from 2000 to 2019 in a nationally representative mortality study. Elife. 2020;9:e54076.
5. Laxme RS, Khochare S, de Souza HF, Ahuja B, Suranse V, Martin G, et al. Beyond the 'big four': venom profiling of the medically important yet neglected Indian snakes reveals disturbing antivenom deficiencies. Plos Negl Trop Dis. 2019;13(12):e0007899.
6. Senji Laxme R, Attarde S, Khochare S, Suranse V, Martin G, Casewell NR, et al. Biogeographical venom variation in the Indian spectacled cobra (*Naja naja*) underscores the pressing need for pan-India efficacious snakebite therapy. Plos Negl Trop Dis. 2021;15(2):e0009150.
7. Senji Laxme R, Khochare S, Attarde S, Suranse V, Iyer A, Casewell NR, et al. Biogeographic venom variation in Russell's viper (*Daboia russelii*) and the preclinical inefficacy of antivenom therapy in snakebite hotspots. Plos Negl Trop Dis. 2021;15(3):e0009247.
8. Rashmi U, Khochare S, Attarde S, Laxme RRS, Suranse V, Martin G, et al. Remarkable intrapopulation venom variability in the monocellate cobra (*Naja kaouthia*) unveils neglected aspects of India's snakebite problem. J Proteomics. 2021;242:104256.
9. Attarde S, Khochare S, Iyer A, Dam P, Martin G, Sunagar K. Venomics of the enigmatic andaman cobra (*Naja sagittifera*) and the preclinical failure of Indian antivenoms in Andaman and Nicobar Islands. Front Pharmacol. 2021;12:768210.
10. Sunagar K, Khochare S, Senji Laxme R, Attarde S, Dam P, Suranse V, et al. A wolf in another wolf's clothing: Post-genomic regulation dictates venom profiles of medically-important cryptic kraits in India. Toxins. 2021;13(1):69.
11. Gopalakrishnan M, Yadav P, Mathur R, Midha N, Garg MK. Venom-induced consumption coagulopathy unresponsive to antivenom after *Echis carinatus sochureki* envenoming. Wilderness Environ Med. 2021;32(2):221–5.
12. Pla D, Sanz L, Quesada-Bernat S, Villalta M, Baal J, Chowdhury MAW, et al. Phylovenomics of Daboia russelii across the Indian subcontinent. Bioactivities and comparative in vivo neutralization and in vitro third-generation antivenomics of antivenoms against venoms from India, Bangladesh and Sri Lanka. Journal of proteomics. 2019;207:103443.
13. Gopal G, Selvaraj H, Venkataramanan SK, Venkataraman S, Saravanan K, Bibina C, et al. Systematic review and meta-analysis on the efficacy

of Indian polyvalent antivenom against the Indian snakes of clinical significance. Arch Toxicol. 2024;98(2):375–93.
14. Patra A, Chanda A, Mukherjee AK. Quantitative proteomic analysis of venom from Southern India common krait (*Bungarus caeruleus*) and identification of poorly immunogenic toxins by immune-profiling against commercial antivenom. Expert Rev Proteomics. 2019;16(5):457–69.
15. Maduwage K, Isbister GK. Current treatment for venom-induced consumption coagulopathy resulting from snakebite. PLoS Negl Trop Dis. 2014;8(10): e3220.
16. Warrell DA. Snake venoms in science and clinical medicine. 1. Russell's viper: biology, venom and treatment of bites. Trans R Soc Trop Med Hyg. 1989;83(6):732–40.
17. Senthilkumaran S, Patel K, Rajan E, Vijayakumar P, Miller SW, Rucavado A, et al. Peripheral arterial thrombosis following Russell's viper bites. TH Open. 2023;7(2):e168–83.
18. Silva A, Maduwage K, Sedgwick M, Pilapitiya S, Weerawansa P, Dahanayaka NJ, et al. Neurotoxicity in Russell's viper (*Daboia russelii*) envenoming in Sri Lanka: a clinical and neurophysiological study. Clin Toxicol (Phila). 2016;54(5):411–9.
19. Subasinghe CJ, Sarathchandra C, Kandeepan T, Kulatunga A. Bilateral blindness following Russell's viper bite - a rare clinical presentation: a case report. J Med Case Rep. 2014;8:99.
20. Madhushani U, Thakshila P, Hodgson WC, Isbister GK, Silva A. Effect of Indian polyvalent antivenom in the prevention and reversal of local myotoxicity induced by common cobra (*Naja naja*) venom from Sri Lanka *in vitro*. Toxins (Basel). 2021;13(5):308.
21. Asad MHHB, McCleary RJR, Salafutdinov I, Alam F, Shah HS, Bibi S, et al. Proteomics study of Southern Punjab Pakistani cobra (*Naja naja*: formerly *Naja naja karachiensis*) venom. Toxicol Environ Chem. 2019;101(1–2):91–116.
22. Faisal T, Tan KY, Tan NH, Sim SM, Gnanathasan CA, Tan CH. Proteomics, toxicity and antivenom neutralization of Sri Lankan and Indian Russell's viper (*Daboia russelii*) venoms. J Venom Anim Toxins Incl Trop Dis. 2021;27:e20200177.
23. Kalita B, Patra A, Das A, Mukherjee AK. Proteomic analysis and immunoprofiling of Eastern India Russell's viper (*Daboia russelii*) venom: correlation between RVV composition and clinical manifestations post RV bite. J Proteome Res. 2018;17(8):2819–33.
24. Tan KY, Tan CH, Fung SY, Tan NH. Venomics, lethality and neutralization of *Naja kaouthia* (monocled cobra) venoms from three different geographical regions of Southeast Asia. J Proteomics. 2015;120:105–25.
25. Mukherjee AK, Kalita B, Mackessy SP. A proteomic analysis of Pakistan *Daboia russelii russelii* venom and assessment of potency of Indian polyvalent and monovalent antivenom. J Proteomics. 2016;144:73–86.
26. Tan NH, Fung SY, Tan KY, Yap MK, Gnanathasan CA, Tan CH. Functional venomics of the Sri Lankan Russell's viper (*Daboia russelii*) and its toxinological correlations. J Proteomics. 2015;128:403–23.
27. Utkin Y, Sunagar K, Jackson TN, Reeks T, Fry BG. Three-finger toxins (3FTxs). In: Fry BG, editor. Venomous Reptiles and Their Toxins: Evolution, Pathophysiology and Biodiscovery. 2015. p. 215–27.
28. Babenko VV, Ziganshin RH, Weise C, Dyachenko I, Shaykhutdinova E, Murashev AN, et al. Novel bradykinin-potentiating peptides and three-finger toxins from viper venom: combined NGS venom gland transcriptomics and quantitative venom proteomics of the Azemiops feae viper. Biomedicines. 2020;8(8):249.
29. Yee KT, Macrander J, Vasieva O, Rojnuckarin P. Newly identified toxin transcripts in Myanmar Russell's viper venom gland. Biol Life Sci Forum. 2023;24(1):11.
30. Doley R, Pahari S, Mackessy SP, Kini RM. Accelerated exchange of exon segments in Viperid three-finger toxin genes (*Sistrurus catenatus edwardsii*; Desert Massasauga). BMC Evol Biol. 2008;8:196.
31. Shelke RR, Sathish S, Gowda TV. Isolation and characterization of a novel postsynaptic/cytotoxic neurotoxin from *Daboia russelli russelli* venom. J Pept Res. 2002;59(6):257–63.
32. Venkatesh M, Prasad N, Sing T, Gowda V. Purification, characterization, and chemical modification of neurotoxic peptide from *Daboia russelii* snake venom of India. J Biochem Mol Toxicol. 2013;27(6):295–304.
33. Fry BG, Undheim EA, Ali SA, Jackson TN, Debono J, Scheib H, et al. Squeezers and leaf-cutters: differential diversification and degeneration of the venom system in toxicoferan reptiles. Mol Cell Proteomics. 2013;12(7):1881–99.
34. Senji Laxme RR, Khochare S, Attarde S, Kaur N, Jaikumar P, Shaikh NY, et al. The Middle Eastern cousin: comparative venomics of *Daboia palaestinae* and *Daboia russelii*. Toxins (Basel). 2022;14(11):725.
35. Oh AMF, Tan CH, Tan KY, Quraishi NH, Tan NH. Venom proteome of *Bungarus sindanus* (Sind krait) from Pakistan and *in vivo* cross-neutralization of toxicity using an Indian polyvalent antivenom. J Proteomics. 2019;193:243–54.
36. Jaglan A, Bhatia S, Martin G, Sunagar K. The Royal Armoury: venomics and antivenomics of king cobra (*Ophiophagus hannah*) from the Indian Western Ghats. Int J Biol Macromol. 2023;253(Pt 2):126708.
37. van Thiel J, Alonso LL, Slagboom J, Dunstan N, Wouters RM, Modahl CM, et al. Highly evolvable: investigating interspecific and intraspecific venom variation in taipans (Oxyuranus spp.) and brown snakes (Pseudonaja spp.). Toxins (Basel). 2023;15(1):74.
38. Colis-Torres A, Neri-Castro E, Strickland JL, Olvera-Rodriguez A, Borja M, Calvete J, et al. Intraspecific venom variation of Mexican West Coast Rattlesnakes (*Crotalus basiliscus*) and its implications for antivenom production. Biochimie. 2022;192:111–24.
39. Sunagar K, Undheim EA, Scheib H, Gren EC, Cochran C, Person CE, et al. Intraspecific venom variation in the medically significant Southern Pacific Rattlesnake (*Crotalus oreganus helleri*): biodiscovery, clinical and evolutionary implications. J Proteomics. 2014;99:68–83.
40. Modahl CM, Roointan A, Rogers J, Currier K, Mackessy SP. Interspecific and intraspecific venom enzymatic variation among cobras (Naja sp. and Ophiophagus hannah). Comp Biochem Physiol C Toxicol Pharmacol. 2020;232:108743.
41. Queiroz GP, Pessoa LA, Portaro FC, Furtado Mde F, Tambourgi DV. Interspecific variation in venom composition and toxicity of Brazilian snakes from *Bothrops* genus. Toxicon. 2008;52(8):842–51.
42. Heptinstall TC, Strickland JL, Rosales-Garcia RA, Rautsaw RM, Simpson CL, Nystrom GS, et al. Venom phenotype conservation suggests integrated specialization in a lizard-eating snake. Toxicon. 2023;229:107135.
43. Zelanis A, de Souza Ventura J, Chudzinski-Tavassi AM, de Fatima Domingues Furtado M. Variability in expression of Bothrops insularis snake venom proteases: an ontogenetic approach. Comp Biochem Physiol C Toxicol Pharmacol. 2007;145(4):601–9.
44. Durban J, Perez A, Sanz L, Gomez A, Bonilla F, Rodriguez S, et al. Integrated "omics" profiling indicates that miRNAs are modulators of the ontogenetic venom composition shift in the Central American rattlesnake. Crotalus simus simus BMC Genomics. 2013;14:234.
45. Durban J, Sanz L, Trevisan-Silva D, Neri-Castro E, Alagon A, Calvete JJ. Integrated venomics and venom gland transcriptome analysis of juvenile and adult Mexican rattlesnakes Crotalus simus, C. tzabcan, and C. culminatus revealed miRNA-modulated ontogenetic shifts. J Proteome Res. 2017;16(9):3370–90.
46. Mackessy SP, Sixberry NM, Heyborne WH, Fritts T. Venom of the Brown Treesnake, *Boiga irregularis*: ontogenetic shifts and taxa-specific toxicity. Toxicon. 2006;47(5):537–48.
47. Madrigal M, Sanz L, Flores-Diaz M, Sasa M, Nunez V, Alape-Giron A, et al. Snake venomics across genus Lachesis. Ontogenetic changes in the venom composition of Lachesis stenophrys and comparative proteomics of the venoms of adult Lachesis melanocephala and Lachesis acrochorda. J Proteomics. 2012;77:280–97.
48. Glaudas X, Jezkova T, Rodriguez-Robles JA. Feeding ecology of the Great Basin rattlesnake (*Crotalus lutosus*, Viperidae). Can J Zool. 2008;86(7):723–34.
49. Schonour RB, Huff EM, Holding ML, Claunch NM, Ellsworth SA, Hogan MP, et al. Gradual and discrete ontogenetic shifts in rattlesnake venom composition and assessment of hormonal and ecological correlates. Toxins. 2020;12(10):659.
50. Mackessy SP. Venom ontogeny in the Pacific rattlesnakes *Crotalus viridis helleri* and *C. v. oreganus*. Copeia. 1988;1988(1):92–101.
51. Gutierrez JM, Avila C, Camacho Z, Lomonte B. Ontogenetic changes in the venom of the snake *Lachesis muta stenophrys* (bushmaster) from Costa Rica. Toxicon. 1990;28(4):419–26.
52. Gutierrez JM, dos Santos MC, Furtado Mde F, Rojas G. Biochemical and pharmacological similarities between the venoms of newborn *Crotalus durissus durissus* and adult *Crotalus durissus* terrificus rattlesnakes. Toxicon. 1991;29(10):1273–7.

53. Saravia P, Rojas E, Arce V, Guevara C, Lopez JC, Chaves E, et al. Geographic and ontogenic variability in the venom of the neotropical rattlesnake *Crotalus durissus*: pathophysiological and therapeutic implications. Rev Biol Trop. 2002;50(1):337–46.
54. Mackessy SP, Leroy J, Mocino-Deloya E, Setser K, Bryson RW, Saviola AJ. Venom ontogeny in the Mexican lance-headed rattlesnake (*Crotalus polystictus*). Toxins (Basel). 2018;10(7):271.
55. Andrade DV, Abe AS. Relationship of venom ontogeny and diet in Bothrops. Herpetologica. 1999;55(2):200–4.
56. Sharma M, Gogoi N, Dhananjaya B, Menon JC, Doley R. Geographical variation of Indian Russell's viper venom and neutralization of its coagulopathy by polyvalent antivenom. Toxin Reviews. 2014;33(1–2):7–15.
57. Sintiprungrat K, Watcharatanyatip K, Senevirathne WD, Chaisuriya P, Chokchaichamnankit D, Srisomsap C, et al. A comparative study of venomics of Naja naja from India and Sri Lanka, clinical manifestations and antivenomics of an Indian polyspecific antivenom. J Proteomics. 2016;132:131–43.
58. Castro-Amorim J, de Novo Oliveira A, Da Silva SL, Soares AM, Mukherjee AK, Ramos MJ, et al. Catalytically active snake venom PLA(2) enzymes: an overview of its elusive mechanisms of reaction. J Med Chem. 2023;66(8):5364–76.
59. Gutiérrez JM, Escalante T, Rucavado A, Herrera C. Hemorrhage caused by snake venom metalloproteinases: a journey of discovery and understanding. Toxins. 2016;8(4):93.
60. Mukherjee AK, Mackessy SP. Biochemical and pharmacological properties of a new thrombin-like serine protease (Russelobin) from the venom of Russell's Viper (*Daboia russelii russelii*) and assessment of its therapeutic potential. Biochimi Biophys Acta (BBA)-General Subjects. 2013;1830(6):3476–88.
61. Takeya H, Nishida S, Miyata T, Kawada S-I, Saisaka Y, Morita T, et al. Coagulation factor X activating enzyme from Russell's viper venom (RVV-X) A novel metalloproteinase with disintegrin (platelet aggregation inhibitor)-like and C-type lectin-like domains. J Biol Chem. 1992;267(20):14109–17.
62. Chen HS, Tsai HY, Wang YM, Tsai IH. P-III hemorrhagic metalloproteinases from Russell's viper venom: cloning, characterization, phylogenetic and functional site analyses. Biochimie. 2008;90(10):1486–98.
63. Du X-Y, Clemetson KJ. Snake venom L-amino acid oxidases. Toxicon. 2002;40(6):659–65.
64. Schonour RB, Huff EM, Holding ML, Claunch NM, Ellsworth SA, Hogan MP, et al. Gradual and discrete ontogenetic shifts in rattlesnake venom composition and assessment of hormonal and ecological correlates. Toxins (Basel). 2020;12(10):659.
65. Kalki Y, Cherukuri S, Adhikari S. Novel prey species in the diet of the spectacled cobra (*Naja naja*). Reptiles Amphibians. 2022;29(1):197–8.
66. Barchan D, Kachalsky S, Neumann D, Vogel Z, Ovadia M, Kochva E, et al. How the mongoose can fight the snake: the binding site of the mongoose acetylcholine receptor. Proc Natl Acad Sci U S A. 1992;89(16):7717–21.
67. Khan MA, Dashevsky D, Kerkkamp H, Kordiš D, de Bakker MA, Wouters R, et al. Widespread evolution of molecular resistance to snake venom α-neurotoxins in vertebrates. Toxins. 2020;12(10):638.
68. Valdujo PH, Nogueira C, Martins M. Ecology of Bothrops neuwiedi pauloensis (Serpentes: Viperidae: Crotalinae) in the Brazilian cerrado. J Herpetol. 2002;37(4):169–76.
69. Rodríguez-Robles JA. Feeding ecology of North American gopher snakes (Pituophis catenifer, Colubridae). Biol J Lin Soc. 2002;77(2):165–83.
70. Thomas RG, Pough FH. The effect of rattlesnake venom on digestion of prey. Toxicon. 1979;17(3):221–8.
71. Kochva E, Nakar O, Ovadia M. Venom toxins: plausible evolution from digestive enzymes. Am Zool. 2015;23(2):427–30.
72. Mackessy SP. Evolutionary trends in venom composition in the western rattlesnakes (Crotalus viridis sensu lato): toxicity vs tenderizers. Toxicon. 2010;55(8):1463–74.
73. Modahl CM, Mukherjee AK, Mackessy SP. An analysis of venom ontogeny and prey-specific toxicity in the Monocled Cobra (*Naja kaouthia*). Toxicon. 2016;119:8–20.
74. Araujo H, Bourguignon S, Boller M, Dias A, Lucas E, Santos I, et al. Potency evaluation of antivenoms in Brazil: the national control laboratory experience between 2000 and 2006. Toxicon. 2008;51(4):502–14.
75. Sunagar K, Jackson TN, Undheim EA, Ali SA, Antunes A, Fry BG. Three-fingered RAVERs: rapid accumulation of variations in exposed residues of snake venom toxins. Toxins (Basel). 2013;5(11):2172–208.
76. Tan NH, Armugam A, Mirtschin PJ. The biological properties of venoms from juvenile and adult taipan (*Oxyuranus scutellatus*) snakes. Comp Biochem Physiol B. 1992;103(3):585–8.
77. Meier J, Freyvogel TA. Comparative studies on venoms of the fer-de-lance (*Bothrops atrox*), carpet viper (*Echis carinatus*) and spitting cobra (*Naja nigricollis*) snakes at different ages. Toxicon. 1980;18(5–6):661–2.
78. Cipriani V, Debono J, Goldenberg J, Jackson TNW, Arbuckle K, Dobson J, et al. Correlation between ontogenetic dietary shifts and venom variation in Australian brown snakes (*Pseudonaja*). Comp Biochem Physiol C Toxicol Pharmacol. 2017;197:53–60.
79. He Y, Gao J, Lin L, Ma X, Ji X. Age-related variation in snake venom: evidence from two snakes (*Naja atra* and *Deinagkistrodon acutus*) in Southeastern China. Asian Herpetol Res. 2014;5(2):119–27.
80. Calvete JJ, Sanz L, Cid P, de la Torre P, Flores-Diaz M, Dos Santos MC, et al. Snake venomics of the Central American rattlesnake *Crotalus simus* and the South American Crotalus durissus complex points to neurotoxicity as an adaptive paedomorphic trend along *Crotalus* dispersal in South America. J Proteome Res. 2010;9(1):528–44.
81. Sousa LF, Nicolau CA, Peixoto PS, Bernardoni JL, Oliveira SS, Portes-Junior JA, et al. Comparison of phylogeny, venom composition and neutralization by antivenom in diverse species of bothrops complex. Plos Negl Trop Dis. 2013;7(9):e2442.
82. Garstang W. The theory of recapitulation: a critical re-statement of the biogenetic law. Zool J Linn Soc. 2008;35(232):81–101.
83. Nunez V, Cid P, Sanz L, De La Torre P, Angulo Y, Lomonte B, et al. Snake venomics and antivenomics of *Bothrops atrox* venoms from Colombia and the Amazon regions of Brazil, Peru and Ecuador suggest the occurrence of geographic variation of venom phenotype by a trend towards paedomorphism. J Proteomics. 2009;73(1):57–78.
84. Borja M, Neri-Castro E, Castañeda-Gaytán G, Strickland JL, Parkinson CL, Castañeda-Gaytán J, et al. Biological and proteolytic variation in the venom of Crotalus scutulatus scutulatus from Mexico. Toxins. 2018;10(1):35.
85. Antunes TC, Yamashita KM, Barbaro KC, Saiki M, Santoro ML. Comparative analysis of newborn and adult *Bothrops jararaca* snake venoms. Toxicon. 2010;56(8):1443–58.
86. Lomonte B, Calvete JJ. Strategies in 'snake venomics' aiming at an integrative view of compositional, functional, and immunological characteristics of venoms. J Venom Anim Toxins Includ Trop Dis. 2017;23:26.
87. Smith BJ. SDS polyacrylamide gel electrophoresis of proteins. Methods Mol Biol. 1994;32:23–34.
88. Schneider CA, Rasband WS, Eliceiri KW. NIH Image to ImageJ: 25 years of image analysis. Nat Methods. 2012;9(7):671–5.
89. Calvete JJ, Lomonte B, Saviola AJ, Calderón Celis F, Ruiz Encinar J. Quantification of snake venom proteomes by mass spectrometry-considerations and perspectives. Mass Spectrom Rev. 2023:1–21. https://doi.org/10.1002/mas.21850. https://analyticalsciencejournals.onlinelibrary.wiley.com/toc/10982787/0/0.
90. Tan NH, Wong KY, Tan CH. Venomics of *Naja sputatrix*, the Javan spitting cobra: A short neurotoxin-driven venom needing improved antivenom neutralization. J Proteomics. 2017;157:18–32.
91. Calvete JJ. Next-generation snake venomics: protein-locus resolution through venom proteome decomplexation. Expert Rev Proteomics. 2014;11(3):315–29.
92. Calvete JJ, Lomonte B, Saviola AJ, Bonilla F, Sasa M, Williams DJ, et al. Mutual enlightenment: a toolbox of concepts and methods for integrating evolutionary and clinical toxinology via snake venomics and the contextual stance. Toxicon X. 2021;9–10:100070.
93. Perez-Riverol Y, Csordas A, Bai J, Bernal-Llinares M, Hewapathirana S, Kundu DJ, et al. The PRIDE database and related tools and resources in 2019: improving support for quantification data. Nucleic Acids Res. 2019;47(D1):D442–50.
94. Freitas-de-Sousa LA, Nachtigall PG, Portes-Junior JA, Holding ML, Nystrom GS, Ellsworth SA, et al. Size matters: an evaluation of the

molecular basis of ontogenetic modifications in the composition of *Bothrops jararacussu* snake venom. Toxins. 2020;12(12):791.
95. Tasoulis T, Lee MS, Ziajko M, Dunstan N, Sumner J, Isbister GK. Activity of two key toxin groups in Australian elapid venoms show a strong correlation to phylogeny but not to diet. BMC Evol Biol. 2020;20(1):1–13.
96. Kishimoto M, Takahashi T. A spectrophotometric microplate assay for L-amino acid oxidase. Anal Biochem. 2001;298(1):136–9.
97. Chowdhury M, Miyoshi S, Shinoda S. Purification and characterization of a protease produced by *Vibrio mimicus*. Infect Immun. 1990;58(12):4159–62.
98. Meléndez-Martínez D, Plenge-Tellechea LF, Gatica-Colima A, Cruz-Pérez MS, Aguilar-Yáñez JM, Licona-Cassani C. Functional mining of the Crotalus Spp. venom protease repertoire reveals potential for chronic wound therapeutics. Molecules. 2020;25(15):3401.
99. Yamashita KM, Alves AF, Barbaro KC, Santoro ML. *Bothrops jararaca* venom metalloproteinases are essential for coagulopathy and increase plasma tissue factor levels during envenomation. Plos Negl Trop Dis. 2014;8(5):e2814.
100. Maisano M, Trapani M, Parrino V, Parisi M, Cappello T, D'Agata A, et al. Haemolytic activity and characterization of nematocyst venom from *Pelagia noctiluca* (Cnidaria: Scyphozoa). Italian J Zool. 2013;80(2):168–76.
101. Teng C-M, Ouyang C, Lin S-C. Species difference in the fibrinogenolytic effects of α-and β-fibrinogenases from *Trimeresurus mucrosquamatus* snake venom. Toxicon. 1985;23(5):777–82.
102. Op den Brouw B, Ghezellou P, Casewell NR, Ali SA, Fathinia B, Fry BG, et al. Pharmacological characterisation of pseudocerastes and eristicophis viper venoms reveal anticancer (melanoma) properties and a potentially novel mode of fibrinogenolysis. Int J Mol Sci. 2021;22(13):6896.
103. Zdenek CN, Harris RJ, Kuruppu S, Youngman NJ, Dobson JS, Debono J, et al. A taxon-specific and high-throughput method for measuring ligand binding to nicotinic acetylcholine receptors. Toxins. 2019;11(10):600.
104. Bracci L, Lozzi L, Lelli B, Pini A, Neri P. Mimotopes of the nicotinic receptor binding site selected by a combinatorial peptide library. Biochemistry. 2001;40(22):6611–9.
105. Mishina M, Tobimatsu T, Imoto K, Tanaka K-I, Fujita Y, Fukuda K, et al. Location of functional regions of acetylcholine receptor α-subunit by site-directed mutagenesis. Nature. 1985;313(6001):364–9.
106. World Health Organisation. Guidelines for the production, control and regulation of snake antivenom immunoglobulins (Revised Second Edition). WHO Technical Report Series, No. 1004, Annex 5. 2017. http://apps.who.int/iris/bitstream/handle/10665/255657/9789241210133-eng.pdf?sequence=1&isAllowed=y#page=217.
107. Finney D. Probit analysis 3rd ed. UK: Cambridge Univ. Press London; 1971.
108. Modahl CM, Mrinalini, Frietze S, Mackessy SP. Adaptive evolution of distinct prey-specific toxin genes in rear-fanged snake venom. Proce Royal Soc B. 1884;2018(285):20181003.
109. Yamasaki T, Narahashi T, Fukaya M, Ishii S, Yamasaki T. Laboratory guide for applied entomologists. Tokyo: Nihon Shokubutsu Boeki Kyokai; 1963.
110. Casewell NR, Cook DA, Wagstaff SC, Nasidi A, Durfa N, Wüster W, et al. Pre-clinical assays predict pan-African Echis viper efficacy for a species-specific antivenom. Plos Negl Trop Dis. 2010;4(10):e851.

Publisher's Note